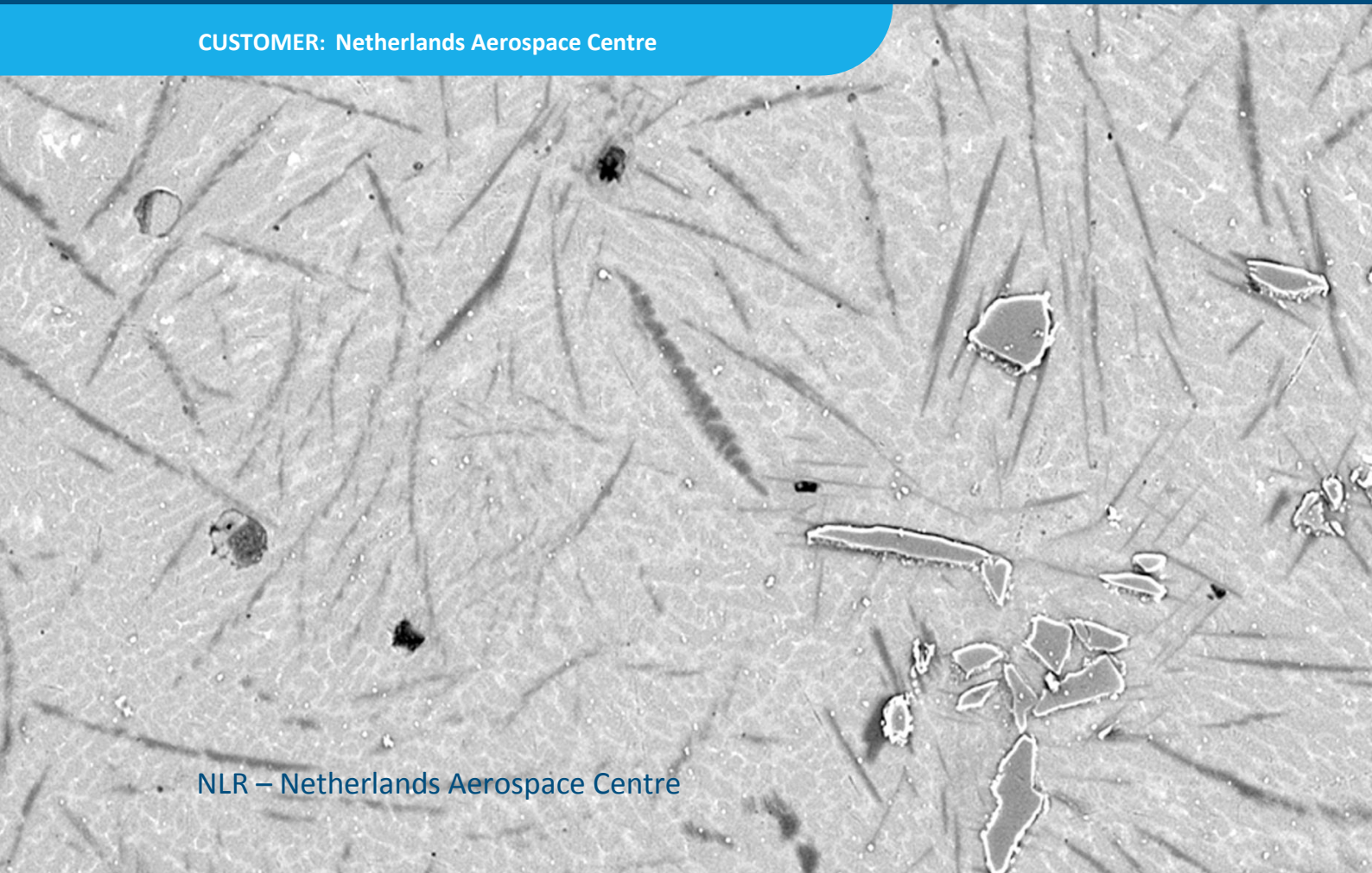




# Review of aeronautical fatigue and structural integrity investigations in the Netherlands during the period March 2015 - March 2017

CUSTOMER: Netherlands Aerospace Centre



NLR – Netherlands Aerospace Centre

	det CBS	mode All	HV ↓ 3.00 kV	mag ↻ 2 500 x	WD 4.8 mm
--	------------	-------------	-----------------	------------------	--------------

20 μm

N.L.R. Multimaterial AM

## Netherlands Aerospace Centre

NLR is a leading international research centre for aerospace. Bolstered by its multidisciplinary expertise and unrivalled research facilities, NLR provides innovative and integral solutions for the complex challenges in the aerospace sector.

NLR's activities span the full spectrum of Research Development Test & Evaluation (RDT & E). Given NLR's specialist knowledge and facilities, companies turn to NLR for validation, verification, qualification, simulation and evaluation. NLR thereby bridges the gap between research and practical applications, while working for both government and industry at home and abroad.

NLR stands for practical and innovative solutions, technical expertise and a long-term design vision. This allows NLR's cutting edge technology to find its way into successful aerospace programs of OEMs, including Airbus, Embraer and Pilatus. NLR contributes to (military) programs, such as ESA's IXV re-entry vehicle, the F-35, the Apache helicopter, and European programs, including SESAR and Clean Sky 2.

Founded in 1919, and employing some 650 people, NLR achieved a turnover of 71 million euros in 2016, of which three-quarters derived from contract research, and the remaining from government funds.

For more information visit: [www.nlr.nl](http://www.nlr.nl)

# Review of aeronautical fatigue and structural integrity investigations in the Netherlands during the period March 2015 - March 2017



*Thermal test of a horizontal stabilizer in an autoclave at Fokker*

## Executive summary

This report is a review of the aeronautical fatigue and structural integrity activities in the Netherlands during the period March 2015 to March 2017. The review is the Netherlands National Delegate's contribution to the 35<sup>th</sup> Conference of the International Committee on Aeronautical Fatigue and Structural Integrity (ICAF) in Nagoya, Japan, on 5 and 6 June 2017.

### REPORT NUMBER

NLR-TP-2017-137

### AUTHOR(S)

M.J. Bos

### REPORT CLASSIFICATION

UNCLASSIFIED

### DATE

April 2017

### KNOWLEDGE AREA(S)

Health Monitoring and Maintenance of Aircraft  
Aerospace Materials  
Aircraft Material and Damage Research  
Aerospace Structures Testing

### DESCRIPTOR(S)

ICAF  
Fatigue  
Structural Integrity  
Damage Tolerance

**GENERAL NOTE**

This report is based on a presentation to be held at the 35<sup>th</sup> Conference of the International Committee on Aeronautical Fatigue and Structural Integrity (ICAF), Nagoya, Japan, June 5-6, 2017.

**NLR**

Anthony Fokkerweg 2

1059 CM Amsterdam

**p**) +31 88 511 3113 **f**) +31 88 511 3210

**e**) [info@nlr.nl](mailto:info@nlr.nl) **i**) [www.nlr.nl](http://www.nlr.nl)



Dedicated to innovation in aerospace

NLR-TP-2017-137 | April 2017

# Review of aeronautical fatigue and structural integrity investigations in the Netherlands during the period March 2015 - March 2017

**CUSTOMER:** Netherlands Aerospace Centre

**AUTHOR(S):**

**M.J. Bos**

NLR

This report is based on a presentation to be held at the 35<sup>th</sup> Conference of the International Committee on Aeronautical Fatigue and Structural Integrity (ICAF), Nagoya, Japan, June 5-6, 2017.

*The contents of this report may be cited on condition that full credit is given to NLR and the authors. This publication has been refereed by the Advisory Committee AEROSPACE VEHICLES.*

<b>CUSTOMER</b>	Netherlands Aerospace Centre
<b>CONTRACT NUMBER</b>	Bestedingsovereenkomst L1414/15
<b>OWNER</b>	Netherlands Aerospace Centre
<b>DIVISION NLR</b>	Aerospace Vehicles
<b>DISTRIBUTION</b>	Unlimited
<b>CLASSIFICATION OF TITLE</b>	UNCLASSIFIED

APPROVED BY :		
AUTHOR	REVIEWER	MANAGING DEPARTMENT
M.J. Bos 	A.A. ten Have 	O.S. Zoetweij 
DATE 180417	DATE 180417	DATE 180417

## Summary

This report is a review of the aeronautical fatigue and structural integrity activities in the Netherlands during the period March 2015 to March 2017. The review is the Netherlands National Delegate's contribution to the 35<sup>th</sup> Conference of the International Committee on Aeronautical Fatigue and Structural Integrity (ICAF) in Nagoya, Japan, on 5 and 6 June 2017.

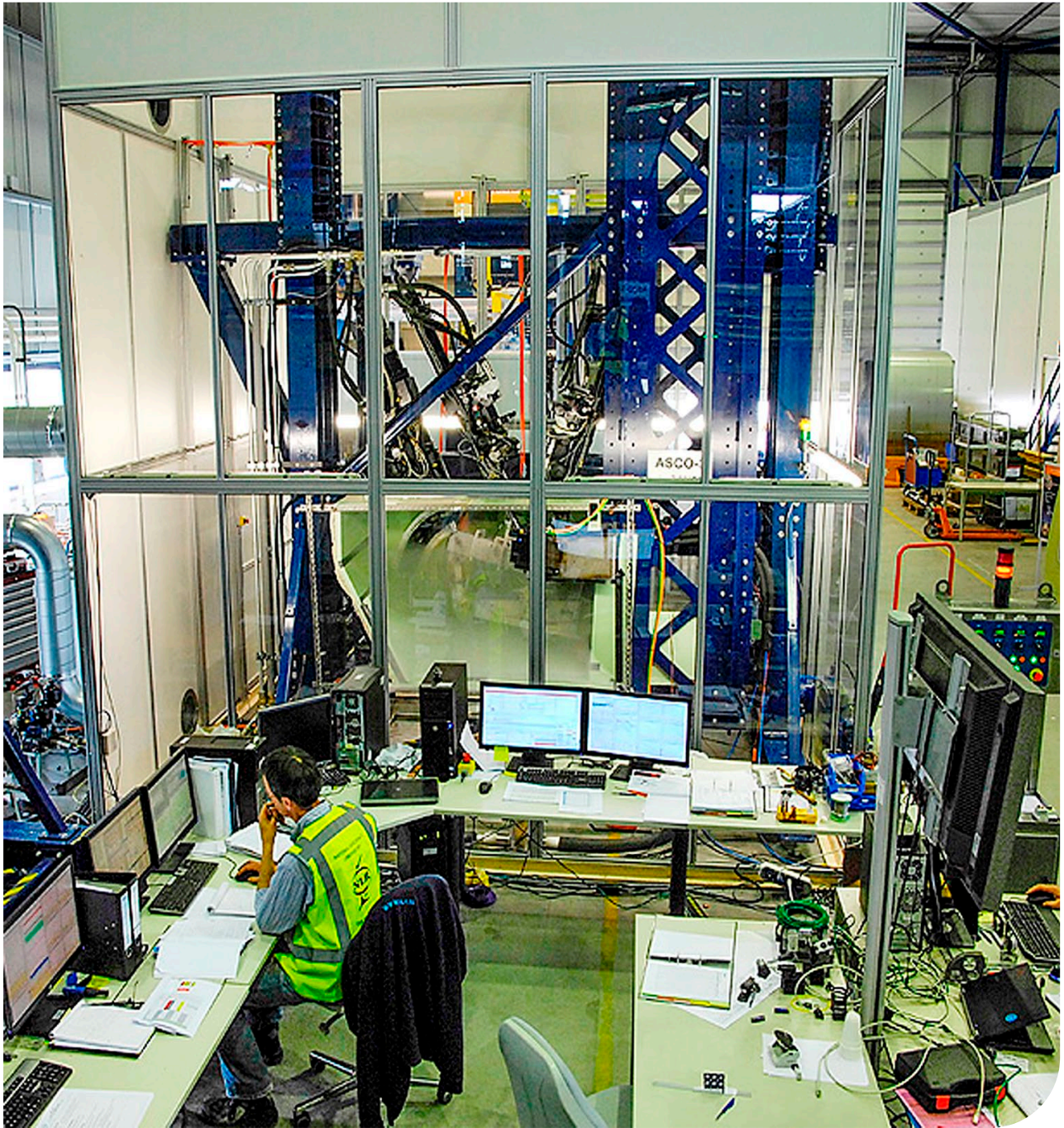


Figure 1: Full scale flap track system test at  $-55^{\circ}\text{C}$  – see section 8.2.

# Contents

<b>Abbreviations</b>	<b>7</b>
<b>1 Introduction</b>	<b>9</b>
<b>2 Metal Fatigue</b>	<b>10</b>
2.1 Towards a proper understanding of fatigue crack growth and crack closure	10
2.2 Prediction of fatigue in engineering alloys (PROF)	12
2.3 Investigation into the influence of build direction on the crack growth behaviour of SLM Ti-6Al-4V	13
<b>3 Adhesively Bonded Interfaces</b>	<b>15</b>
3.1 Characterisation of fatigue crack growth in adhesive bonds	15
3.2 Failure of adhesively-bonded metal-skin-to-composite-stiffener: effect of temperature & cyclic loading	16
3.3 Central cut ply specimens for characterizing Mode II fatigue disbond growth: a critical evaluation	18
3.4 Monitoring surface contamination of post peel test metal-metal bonded interfaces using hyperspectral imaging	19
<b>4 Composites &amp; Fibre Metal Laminates</b>	<b>20</b>
4.1 Multiple-Site Damage crack growth behaviour in Fibre Metal Laminate structures	20
4.2 Assessment of the fatigue and quasi-static damage directionality in Fibre Metal Laminates	21
4.3 Thermal strains in heated Fibre Metal Laminates	22
4.4 Assessing the contribution of the process zone ahead of the mode II delamination tip in CFRP laminates	23
<b>5 Prognostics &amp; Risk Analysis</b>	<b>25</b>
5.1 Real-time fatigue life prognostics of composite structures using stochastic modelling and SHM data	25
5.2 Probabilistic life prediction model for welded structures	26
5.3 Thermal loads in a business jet horizontal stabilizer	27
<b>6 Non-Destructive Evaluation</b>	<b>33</b>
6.1 Near-infrared optical coherence tomography for inspection of fibre composites	33
6.2 Evaluating delamination growth in composites under dynamic loading using infrared thermography	33
6.3 Analysis of chemical degradation of thermally cycled glass-fibre composites using hyperspectral imaging	34
6.4 In-service ultrasonic detection of impact damage in thick-walled composites	35
6.5 In-service inspection of water ingress in composite honeycomb structures	37
<b>7 Structural Health &amp; Usage Monitoring</b>	<b>38</b>
7.1 Fielding a Structural Health Monitoring system on legacy military aircraft: a business perspective	38
7.2 Modal Strain Energy based Structural Health Monitoring of rib stiffened composite panels	39
7.3 Experimental evaluation of vibration-based identification of damage in a composite aircraft structure with internally-mounted piezodiaphragm sensors	41
7.4 Individual tracking of RNLAf aircraft	42
7.5 Towards condition based maintenance of drive train components of aging military helicopters	43

<b>8</b>	<b>Advanced Testing</b>	<b>45</b>
8.1	Advanced multi-axial testing of thermoplastic carbon composite laminates	45
8.2	Full-scale endurance testing of flap tracks at low temperatures	46
8.3	Certification test activity for a hybrid structure	48
<b>9</b>	<b>Fleet Life Management</b>	<b>51</b>
9.1	Multi-nation NH90 Supportability Data Exchange	51
9.2	Roadmap to Condition Based Maintenance	51
9.3	Experimental investigation of damage tolerance substantiation methods for hybrid structures	53
<b>10</b>	<b>Special Category</b>	<b>55</b>
10.1	Fatigue and fracture of Fibre Metal Laminates	55
10.2	Biaxial fatigue of metals – the present understanding	55
10.3	Portable Impactor	55
10.4	Delft Workshop on Physics of Fatigue Damage Growth	56
10.5	Milestone case histories in aircraft structural integrity	56
	<b>References</b>	<b>57</b>

# Abbreviations

ACRONYM	DESCRIPTION
AE	Acoustic Emission
AM	Additive Manufacturing
ASIP	Aircraft Structural Inspection Program
CA	Constant Amplitude
CBM	Condition Based Maintenance
CFRP	Carbon Fibre Reinforced Polymer
CRES	Corrosion Resistant Steel
CVFDR	Cockpit Voice and Flight Data Recorder
DIC	Digital Image Correlation
DST-G	Defence Science and Technology Group, Australia
EASA	European Aviation Safety Agency
ELS	End Loaded Split
ENF	End Notch Flexure
FAA	Federal Aviation Administration
FALSTAFF	Fighter Aircraft Loading STandard For Fatigue Evaluation
FCG	Fatigue Crack Growth
FDT	Fatigue and Damage Tolerance
FEM	Finite Element Model, Finite Element Method
FML	Fibre Metal Laminate
GAG	Groun-Air-Ground cycle
GARTEUR	Group for Aeronautical Research and Technology in Europe
GFRP	Glass Fibre Reinforced Polymer
HIP	Hot Isostatic Pressing
HSI	HyperSpectral Imaging
IAT	Individual Aircraft Tracking
ICAF	International Committee on Aeronautical Fatigue and Structural Integrity
ISA	International Standard Atmosphere
JAMS	Joint Advanced Materials and Structures Center of Excellence (FAA)
LEF	Load Enhancement Factor
LEFM	Linear Elastic Fracture Mechanics
LID	Load Introduction Device
LLS	Load-Life Shift
MSD	Multi-Site Damage
MSE, MSE-DI	Modal Strain Energy, Modal Strain Energy Damage Index
MTBF	Mean Time Between Failure

NAHEMA	NATO Helicopter Management Agency
NDI	Non-Destructive Inspection
NIAR	National Institute for Aviation Research
NLR	Netherlands Aerospace Centre
OCT	Optical Coherence Tomography
OEM	Original Equipment Manufacturer
PEFR	Pulse-Echo Flaw Reflection
PHM	Prognostics and Health Management
PROF	PRediction Of Fatigue in engineering alloys
QF	Quantitative Fractography
R	Stress ratio
RAM	Reliability, Availability, Maintainability
RNLAF	Royal Netherlands Air Force
RT	Room Temperature
RTM	Resin Transfer Moulding
RUL	Remaining Useful Life
SDE	Supportability Data Exchange
SER	Strain Energy Release
SHM	Structural Health Monitoring
SIF	Stress Intensity Factor
SLM	Selective Laser Melting
SR	Stress Relieved
TOF	Time Of Flight
TRL	Technology Readiness Level
TU Delft	Delft University of Technology
UD	Uni-Directional
UHCF	Ultra High Cycle Fatigue
UT, UT-PA	Ultrasonic Testing, Ultrasonic Testing – Phased Array
VA	Variable Amplitude
WFD	Widespread Fatigue Damage
WMC	Wind turbine Materials and Constructions

# 1 Introduction

The present review gives a summary of the work performed in the Netherlands in the field of aeronautical fatigue and structural integrity during the period from March 2015 to March 2017. The contributions to this review come from the following sources:

- Delft University of Technology (TU Delft)
- Fokker Aerostructures
- Knowledge Centre Wind turbine Materials and Constructions (WMC)
- Netherlands Aerospace Centre (NLR)
- Royal Netherlands Air Force (RNLAf)
- University of Twente.

In addition, collaborative work between NLR and the Defence Science and Technology Group (DST-G) of Australia is included.

The names of the principal investigators and their affiliations are given at the start of each topic. The format and arrangement of this review is similar to that of previous years.

## 2 Metal Fatigue

### 2.1 Towards a proper understanding of fatigue crack growth and crack closure

Joël Hogeveen, René Alderliesten, TU Delft

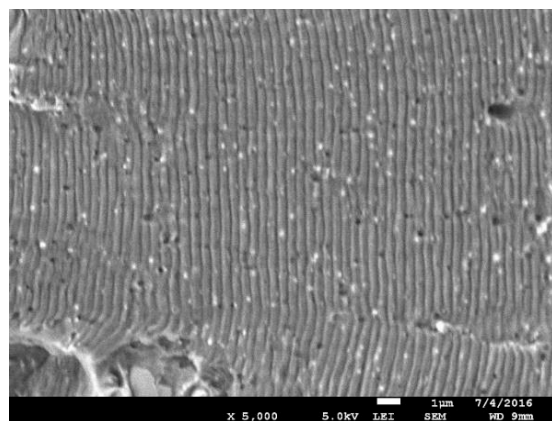
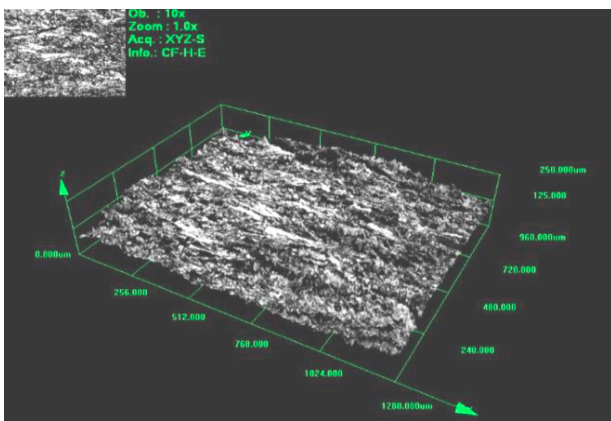
Conventional theories to describe and predict FCG are based on a SIF parameter,  $\Delta K$ . If  $\Delta K$  is used as similitude parameter to predict FCG, an R-effect arises. This R-effect can be accounted for by means of plasticity induced crack closure: A plastic wake behind the crack tip causes the crack to close before a zero tensile load is applied.  $\Delta K$  is therefore adapted to an effective  $\Delta K$ ,  $\Delta K_{\text{eff}}$ . If  $\Delta K_{\text{eff}}$  is used for similitude the R-effect disappears. These theories have recently been disputed and an alternative, SER dominated FCG description model has been proposed. This research discusses the confusion about using  $\Delta K$  for similitude and approaches FCG also from a SER perspective.

Fatigue crack growth experiments were designed and executed in lab-air and vacuum environment to obtain a better understanding of fatigue, the R-effect and crack closure. R-values were applied in a range from 0.02 to 0.5. The following observations were made:

- The amount of plasticity, i.e. plastic zone size, in both air and vacuum is similar.
- The transition point to non-linearity in the load versus crack opening displacement curve is only observed for low R-values; when  $S_{\text{min}}$  is above this level, the non-linearity disappears.
- The transition point is independent of environment, the stress ratio R and the crack length, but is observed to depend on  $S_{\text{max}}$ .
- The fracture surface roughness is different and develops differently for lab-air and vacuum.
- Correcting the crack surface for this roughness brings the characteristic trend of  $dU/dN = dU/dA \cdot dA/dN$  for both environments closer together.

In summary, the experimental results show that  $\Delta K$  is an improper similitude parameter and that the R-effect is an artefact of choosing  $\Delta K$  for similitude. Instead of that, fatigue should be approached from a SER perspective. Furthermore the research shows that the R-effect is not caused by (plasticity induced) crack closure.

The MSc thesis that contains the results of this study can be downloaded from the repository of TU Delft – see ref. [1].



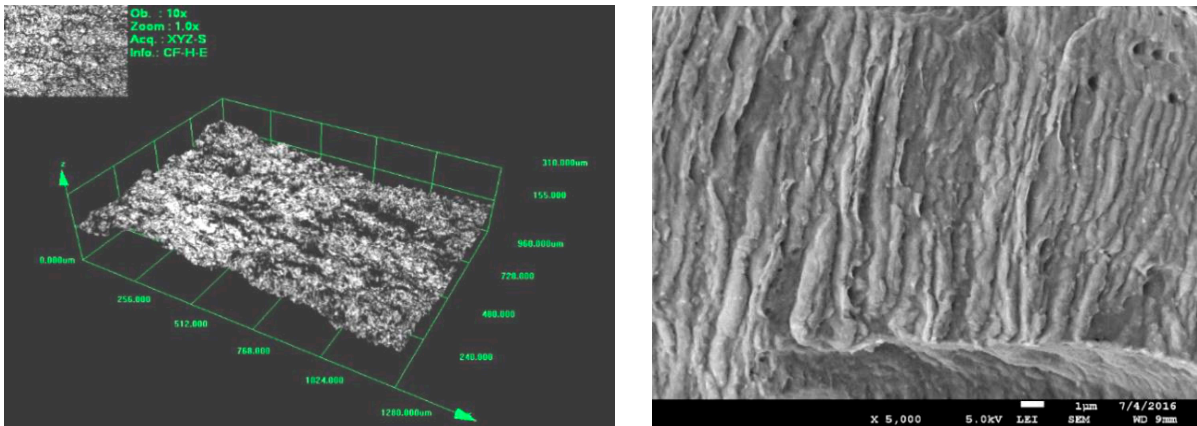


Figure 2: Differences in fracture surfaces created in lab-air (top) and vacuum (bottom) at  $a = 11$  mm, in specimens tested at  $S_{max} = 75$  MPa,  $R = 0.1$ .

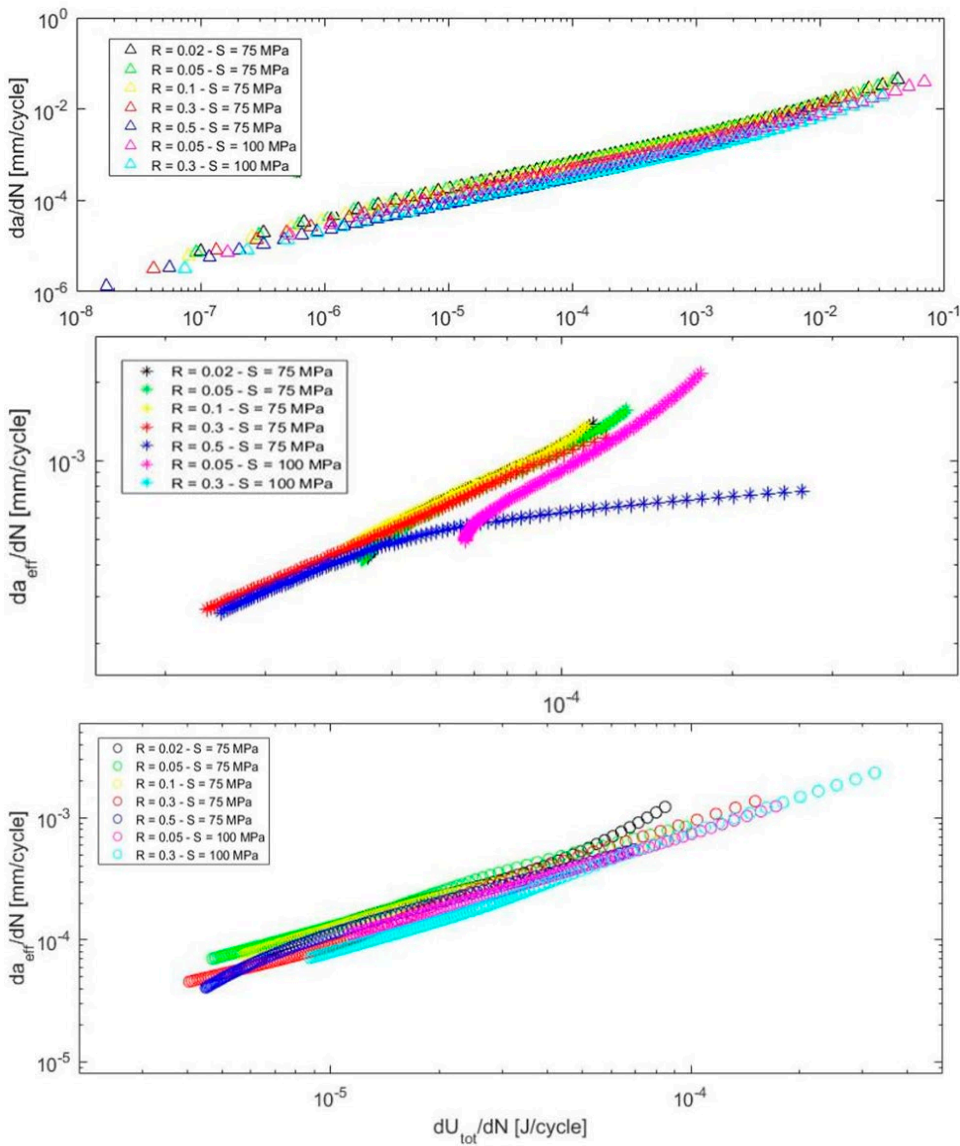
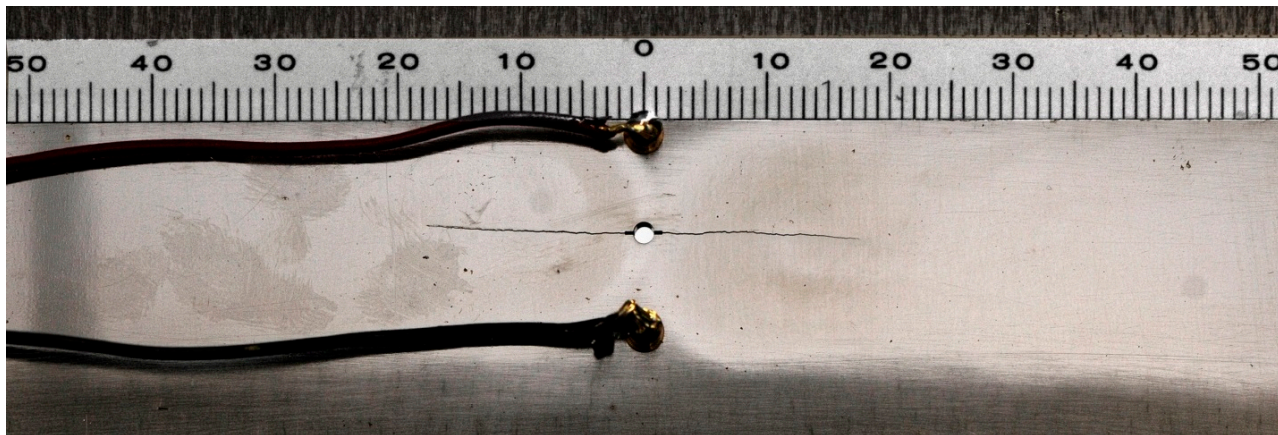


Figure 3: Striking correlation between  $dU/dN = dU/dA * dA/dN$  trends after correction of surface roughness: numerical prediction (top), lab-air (centre), and vacuum (bottom).

## 2.2 Prediction of fatigue in engineering alloys (PROF)

*Emiel Amsterdam, NLR*

The objective of the project “Prediction of fatigue in engineering alloys (PROF)” is to improve the understanding and prediction of fatigue in aluminium and steel alloys. This four year NLR project was started in 2016/Q3. It is conducted in collaboration with Fokker, Embraer, Wartsilä, TU Delft and the Royal Netherlands Air Force.



*Figure 4: Measurement of crack length in a AA 7075-T7351 M(T) specimen.*

In 2015 NLR has demonstrated that for 29 identical fatigue crack growth tests on aluminium alloy 7075-T7351 M(T) specimens the exponent of the Paris law changes between specimens and crack lengths. Fractography and crack length measurements show that the exponent is higher and varies at crack lengths where crack growth is dominated by plane strain conditions. The power law exponent decreases and is similar for all specimens after the transition to plane stress conditions at higher crack lengths. The mathematical concept of a pivot point is used to model crack growth with two different exponents using a dimensionally correct equation. It also allows to model the crack growth variation in all specimens by varying only one parameter, the power law exponent for the plane strain condition [2], which is a relevant observation for structural risk analyses.

PROF will extend the previous research to include the effect of stress amplitude, thickness, test conditions and variable amplitude loading on the fatigue crack growth rate. Initially the research is focussed on AA 7075-T7351. At a later stage other engineering materials will be considered as well, such as other aluminium alloys, structural and high strength steels. Specific interest is present for crack growth below the (long crack) threshold, also indicated as short crack growth. This is also applicable to ultra high cycle fatigue (UHCF), where it is unknown how many cycles are consumed in nucleation and the short crack growth phase. Quantitative fractography (QF) and marker loads will be used to determine the crack growth rate during this phase. This should lead to improved physics based knowledge on fatigue crack growth. This knowledge will ultimately allow for better alloy development, more accurate calculation of lifetime or inspection intervals and less testing in the future when, for example, the loading spectrum changes. The effect of VA loading on fatigue is modelled by a PhD-student from TU Delft. The initial CA fatigue crack growth rate test on AA 7075-T7351 M(T) specimens show that it is possible to exactly model the fatigue crack growth of each specimen from an electro discharge machining starter notch to final failure with multiple power law exponents at different crack length ranges using a dimensionally correct equation - see Figure 5.

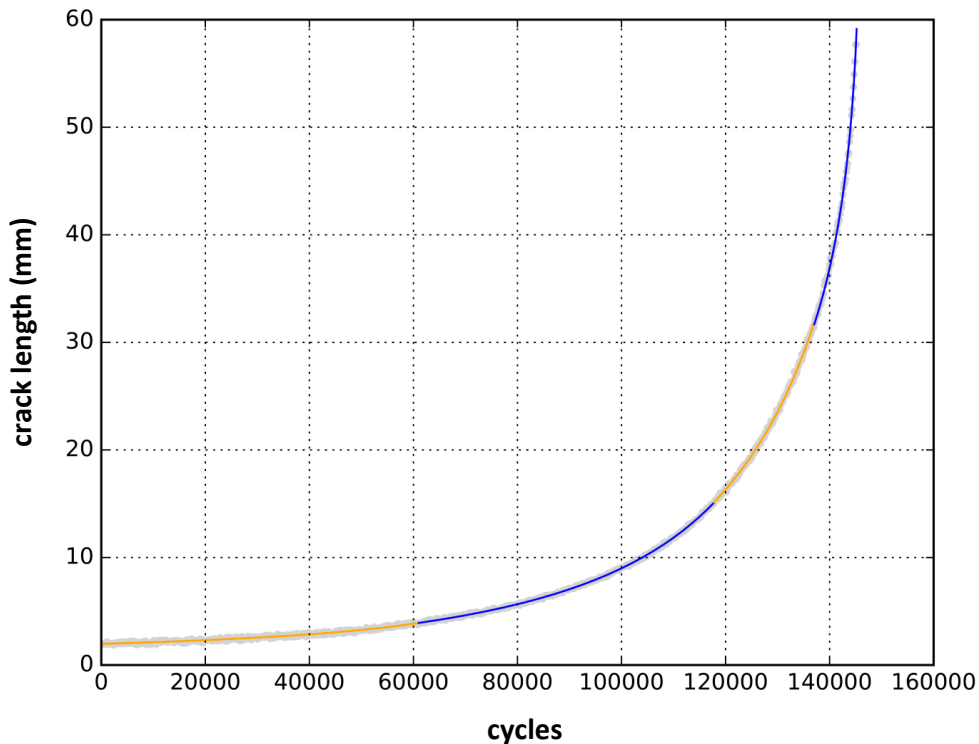


Figure 5: Crack length vs. cycles for a AA 7075-T7351 M(T) specimen. The experimental curve is exactly modelled using different power law exponents for four crack length ranges (indicated by the orange and blue lines).

## 2.3 Investigation into the influence of build direction on the crack growth behaviour of SLM Ti-6Al-4V

Jef Michielssen, Calvin Rans, TU Delft

The aim of this research was to investigate the effect of a varying build orientation and different heat treatment on the crack propagation properties of SLM Ti-6Al-4V. Both crack propagation rate and direction were considered.

Fatigue tests have been performed with a constant cyclic load and single edge notch specimens. Ten unique types of specimens were tested by combining five different build orientation (0°, 30°, 45°, 60° and 90°) with two different heat treatments (Stress Relieved and Hot Isostatic Pressing). In the end, similar crack propagation rates were measured for all specimens, see Figure 6. Although small differences were seen in the microstructure and DIC analysis, they did not seem to change the crack propagation rate. This observation led to the conclusion that the crack propagation rate is not influenced by a change in build orientation or a change in heat treatment.

On the other hand, the measured crack paths showed some differences. Small crack deflections were found for 30° - SR and 45° & 60° - HIP, while all other specimens had cracks propagating in a direction normal to the applied stress. As only off-axis specimens showed repetitive crack deflections, it can be concluded that the anisotropic microstructure is causing this behaviour. However, no conclusive explanation could be given based on the data gathered in this experiment. It is expected that different mechanisms caused the crack deviations as it happened in both heat treatments but for different orientations. Further research in this specific field is needed to explain the measured behaviour.

The MSc thesis that contains the results of this study can be downloaded from the repository of TU Delft – see ref. [3].

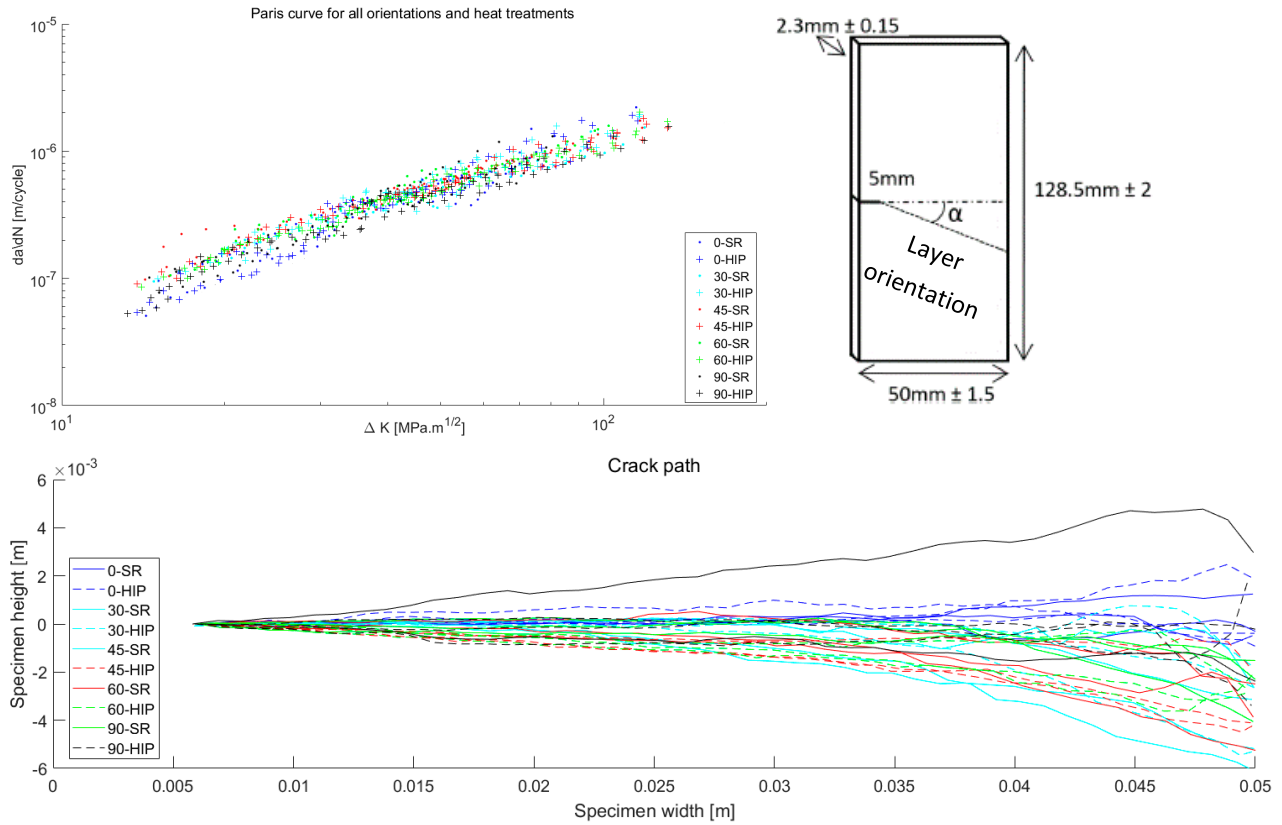


Figure 6: Paris curves for all orientations and heat treatments generated with the illustrated sample (upper), and observed crack paths (bottom).

## 3 Adhesively Bonded Interfaces

### 3.1 Characterisation of fatigue crack growth in adhesive bonds

John-Alan Pascoe, René Alderliesten, Rinze Benedictus, TU Delft

Although there is quite a collection of models available in the literature for the prediction of fatigue crack growth in adhesive bonds, these models are invariably based on empirical curve-fits. The consequence is that the limit of validity of these models is not always clear, and that extensive test campaigns are necessary in order to generate the data necessary to calibrate these models. In order to develop more accurate models, a better understanding of the physics of crack growth is required. This research represents an attempt to generate this understanding, by characterising the crack growth in terms of the strain energy dissipation.

Measuring the force ( $P$ ) and displacement ( $d$ ) during a fatigue test allows the strain energy in the specimen to be determined. By measuring the strain energy repeatedly, the energy dissipation per cycle  $dU/dN$  can be found. This can then be compared to the crack growth rate  $da/dN$ .

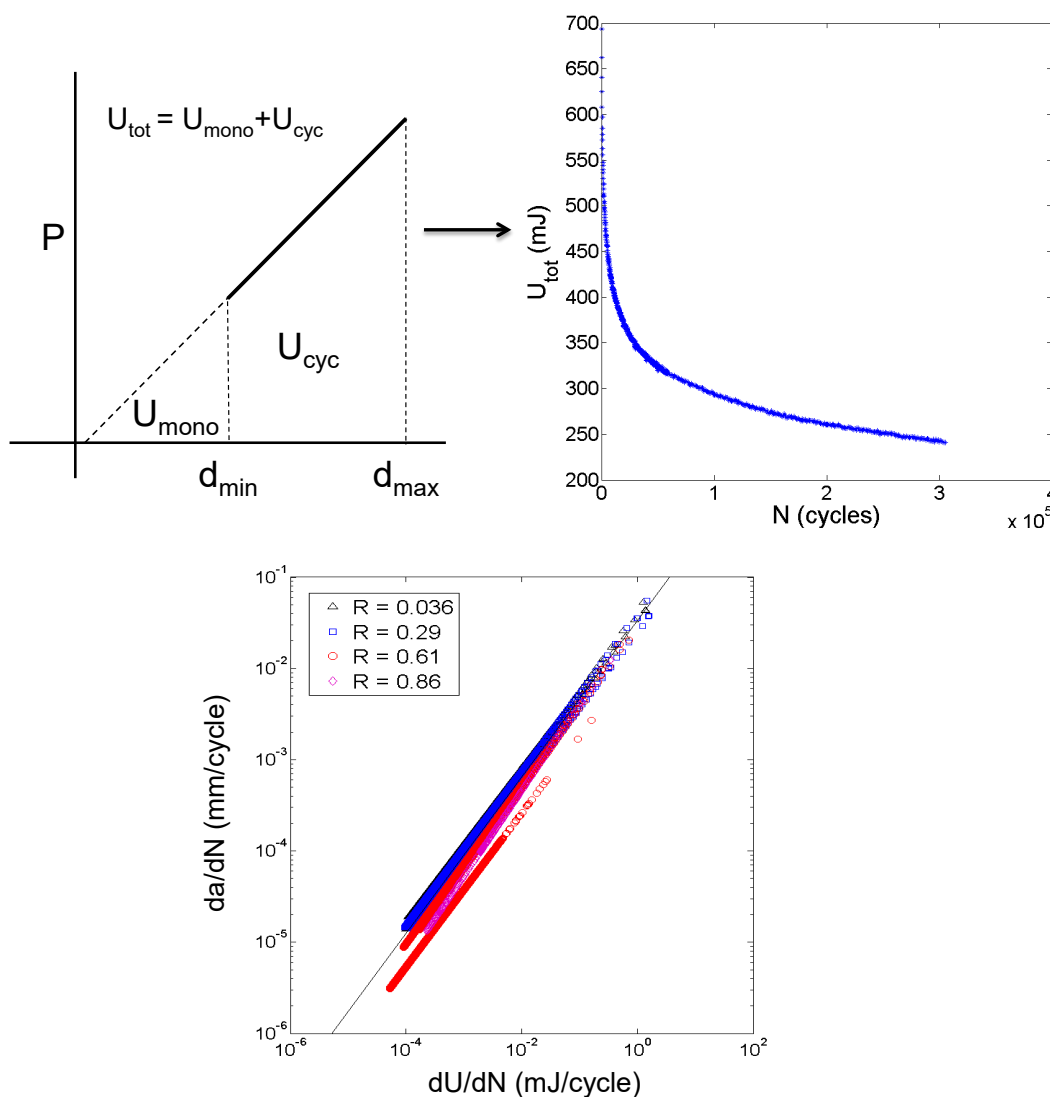


Figure 7: Illustration of the concept to characterize fatigue damage growth with  $dU/dN = dU/da * da/dN$ .

Furthermore one can determine the average energy dissipation per unit of crack growth:

$$G^* = \frac{1}{w} \frac{dU/dN}{da/dN}$$

where  $w$  is the specimen width. Since  $G^*$  indicates how much energy is required per unit of crack growth, it can be interpreted as the resistance to crack growth. On the other hand,  $dU/dN$  indicates the total amount of energy dissipated in a given cycle. Therefore it is a measure for the amount of energy available for crack growth in that cycle. It was found that the amount of required energy correlates to the maximum load (in terms of maximum strain energy release rate (SERR)  $G_{max}$ ). The amount of available energy was found to correlate to the load range (in terms of  $\Delta G$  or  $\Delta K$ ) and/or the applied work  $U_{cyc}$ .

The findings of this work have been published in a PhD thesis [4]. A summary of the main conclusions is also provided in a recently published article, which also highlights how the findings described above can be used to qualitatively explain the R-ratio effect [5]. The data produced during this research project is publically available [6].

## 3.2 Failure of adhesively-bonded metal-skin-to-composite-stiffener: effect of temperature & cyclic loading

*Sofia Teixeira de Freitas, Jos Sinke, TU Delft*

The aim of this research was to analyse the failure mechanisms of a Fibre Metal Laminate (FML) skin adhesively bonded to a Carbon Fibre Reinforced Polymer (CFRP) stiffener, under quasi-static loading at different environmental temperatures ( $-55$  °C, Room Temperature RT and  $+100$  °C) and under fatigue loading at RT. Stiffener pull-off tests were performed to simulate full-scale components subject to out-of-plane loading.

The damage initiation and propagation is similar under quasi-static loading and fatigue loading. The crack initiates at the CFRP stiffener noodle and propagates through the CFRP stiffener foot plies and web plies. No disbond was detected at the bond line in any of the quasi-static and fatigue tests. Figure 8 shows the typical failure sequence: (1) damage initiation at the noodle of the CFRP stiffener; (2) damage propagation by delamination from the noodle to the stiffener foot; (3) detachment of the stiffener from the skin. The fatigue life initiation of the bonded structures presents a very large scatter. The stress level at the stiffener noodle may present a significant scatter due to initial manufacturing defect yielding to a scatter in the crack initiation. Nevertheless, the fatigue life propagation presents more stable results which may allow for a good prediction and a damage tolerant design.

Figure 9 shows typical fracture surfaces under quasi-static loading. The main failure mechanism at the CFRP stiffener is mixed mode I/II delamination, both under static and fatigue loading. The fracture morphology indicates that the mechanics of crack initiation are the same under static and fatigue loading. Flake-like shear cusps are a typical feature in the fracture surface of mixed mode I/II delamination at high temperatures (above RT), opposite to cusps with serrated feet at lower temperatures. Under fatigue loading at the crack propagation area, the typical fracture morphology are rolled cusps – Figure 9.

More information is provided in ref. [7].

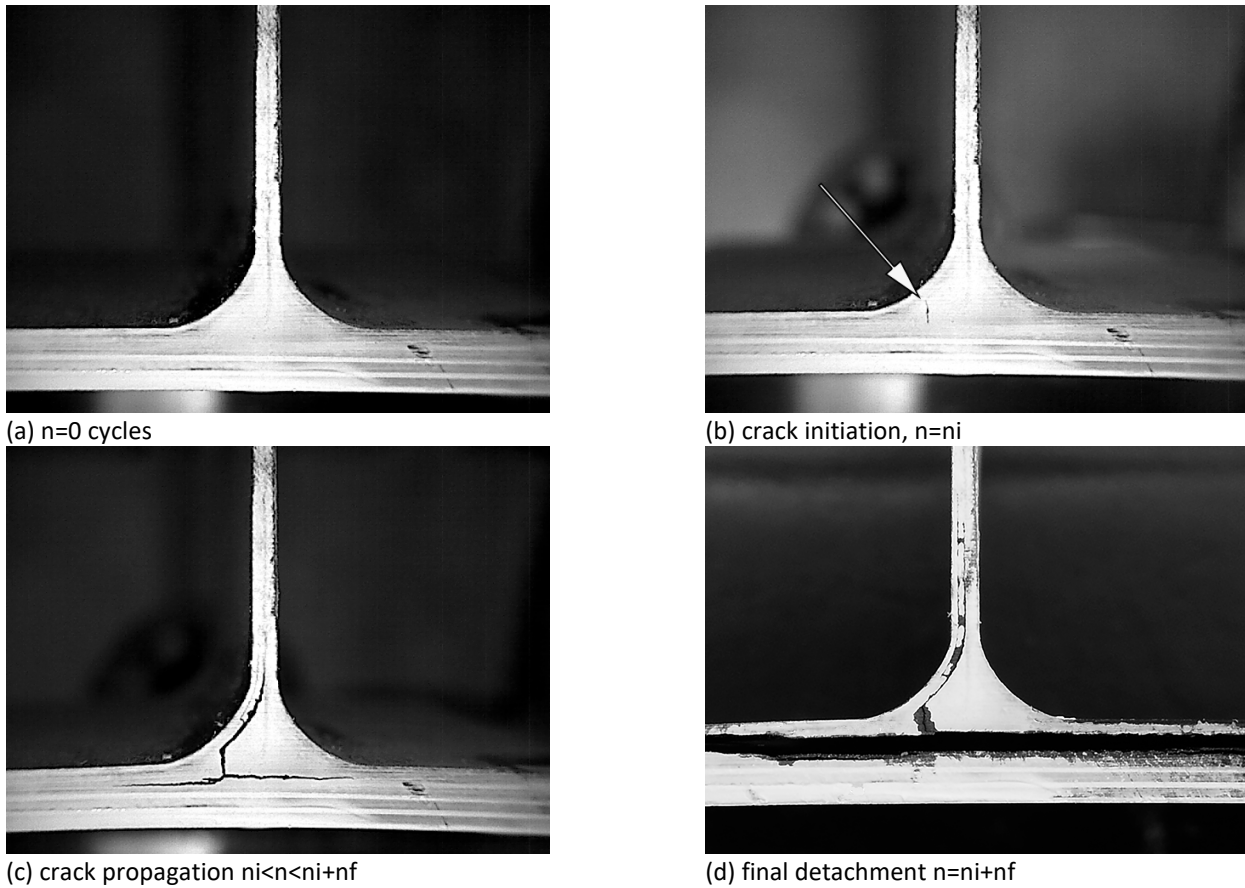


Figure 8: Typical fatigue damage events ( $n$  – number of fatigue cycles;  $n_i$  – number of cycles to crack initiation – fatigue life initiation;  $n_f$  – number of cycles from crack initiation to complete detachment – fatigue life propagation).

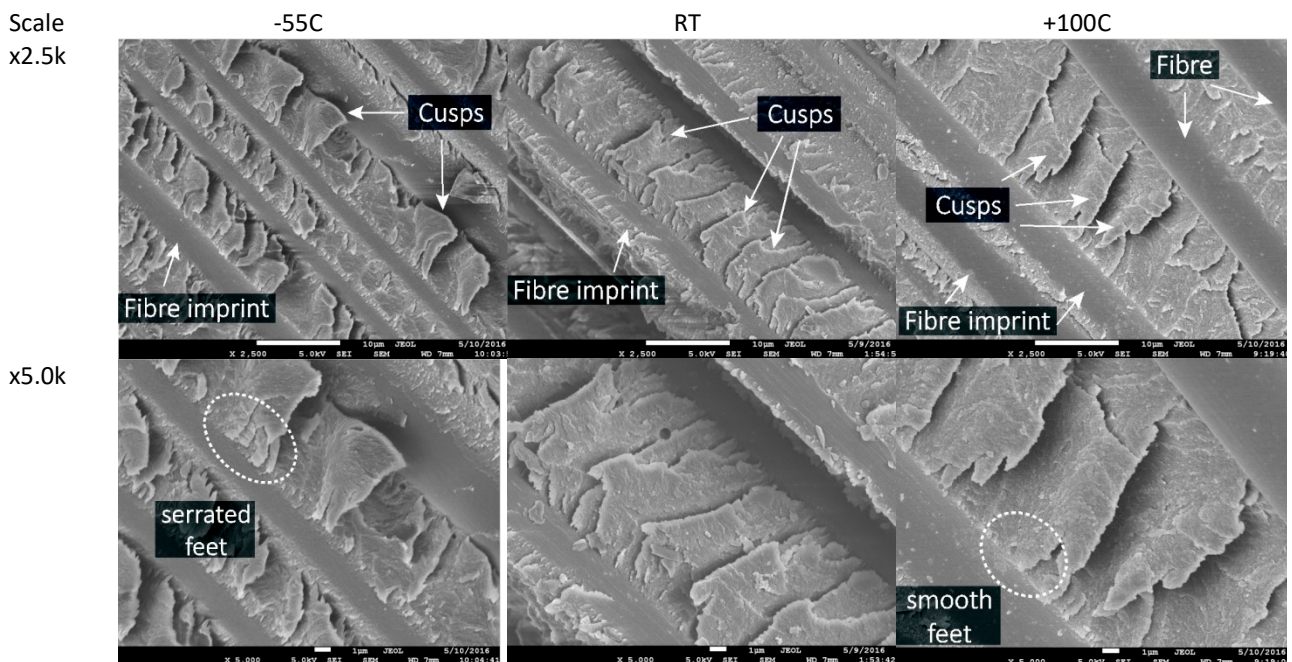


Figure 9: Typical quasi-static fracture surfaces at the area of crack propagation on the stiffener foot plies.

### 3.3 Central cut ply specimens for characterizing Mode II fatigue disbond growth: a critical evaluation

*Fabricio Ribeiro, Marcias Martinez, Calvin Rans, Rinze Benedictus, TU Delft*

The lack of a widely-accepted test standard for characterizing the fatigue disbond growth behaviour of adhesively bonded interfaces is a challenge to the research community in terms of producing consistent and repeatable results. Typically, researchers apply specimen configurations such as the End Notch Flexure (ENF) and End Loaded Split (ELS) which are widely used for studying the static crack growth behaviour of bonded interfaces. However, the needs for static and fatigue disbond growth characterization are not the same, resulting in some undesirable effects in such specimens. This study looks at a particular test configuration – the central cut ply specimen – that has been gaining traction for fatigue disbond growth characterization. A critical evaluation of the suitability of this specimen, including the influence of geometry, disbond measurement approaches, and the stability of the disbond growth is carried out through a combination of numerical and experimental investigations. Results of this evaluation (see Figure 10) have shown that, indeed, the central cut ply specimen is a promising specimen configuration for characterizing fatigue disbond growth; however, it also presents several challenges that require consideration in its application.

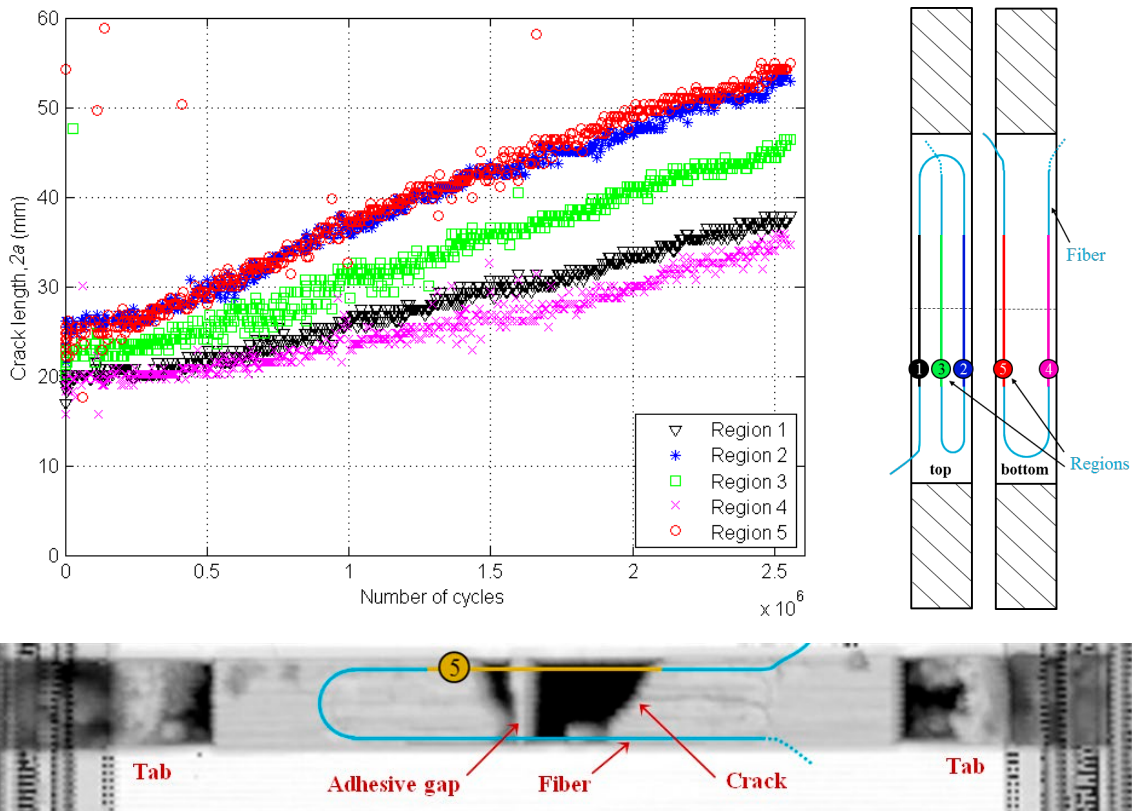


Figure 10: Crack growth behaviour observed under constant amplitude loading with a fibre optic distributed sensing system; C-scan image of disbond shown for comparison.

### 3.4 Monitoring surface contamination of post peel test metal-metal bonded interfaces using hyperspectral imaging

V. M. Papadakis, S. Teixeira de Freitas, R. M. Colijn, J. J. Goedhart, J. A. Poulis, R. M. Groves, TU Delft

The adhesion process of bonded structures is a very sensitive manufacturing process, in particular to surface contamination. Nowadays, the adhesion quality of bonded joints can only be detected by destructive testing such as peel tests. But, for actual structures destructive testing of every bonded part is obviously not an option and industry is lacking a non-destructive test to quantify adhesion strength. In this work a methodology is described that could lead to a successful detection of possible contamination agents during the manufacturing process of bonded structures. Hyperspectral imaging is an optical non-destructive technique that allows mapping of specific chemical characteristics of a surface in high contrast, already applied in astronomy, remote sensing and medical sciences. In this work multiple sets of aged and non-aged adhesively bonded specimens was studied: aluminium-to-aluminium using standard floating roller peel test (ASTM D3167). After destructive testing, the contamination level of the fracture surfaces of the bonded specimens was studied using a line-scan hyperspectral imaging system (ImSpector V10E spectrograph, SPECIM, Finland), see in Figure 11 (a). This system is capable of acquiring reflectance data in the 400-1000 nm range with a bandwidth of 2.8 nm. Three 30 W tungsten halogen light sources provided uniform illumination across all the sensitivity range of the sensor. The resulting images of each specimen had a resolution of 1312 \* 300 pixels, with an exposure time of 200 msec. Following acquisition, all measurements were normalized with the use of a white diffuse reference target. Reference reflectance spectra were extracted from suspicious areas and a non-negative-least-square un-mixing algorithm was applied to check for chemical similarities. Two main signals were detected and mapped onto the surfaces. Statistical analysis was performed, based on the mapping results that described the surface percentage coverage of the contaminant signals and the related statistical errors, followed by the reference component analysis (RCA), shown in Figure 11(b). A correlation between the percentage of contamination and the adhesive failure was found.

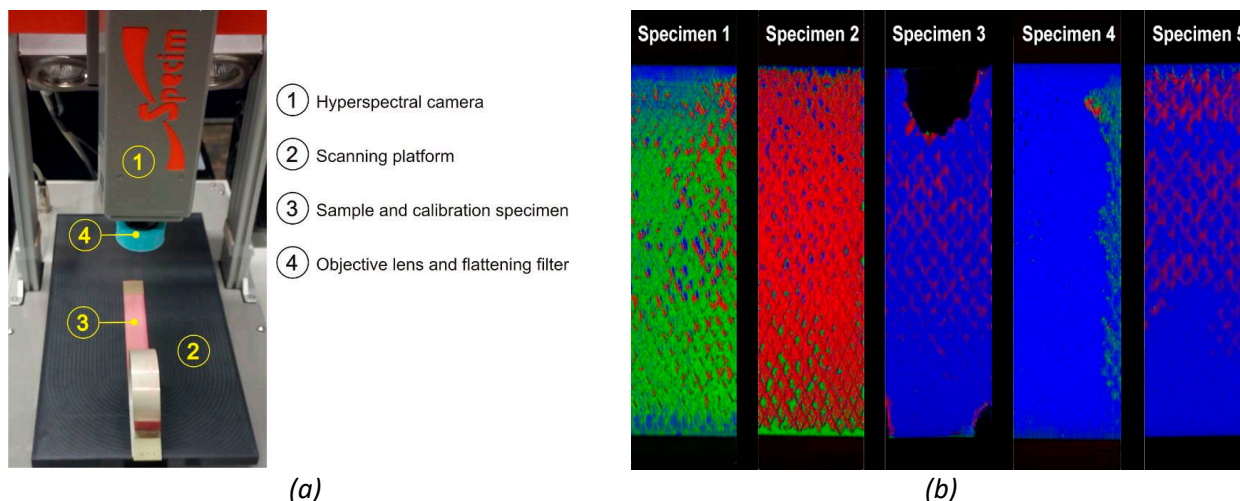


Figure 11: (a) photo of the laboratory hyperspectral imaging setup and (b) RCA resulting pseudo-color images from five peel test specimens subjected to different environmental conditions.

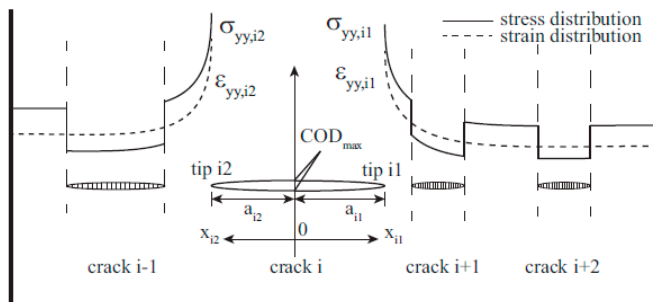
This work has been presented at SPIE Europe, Brussels, in April 2016.

## 4 Composites & Fibre Metal Laminates

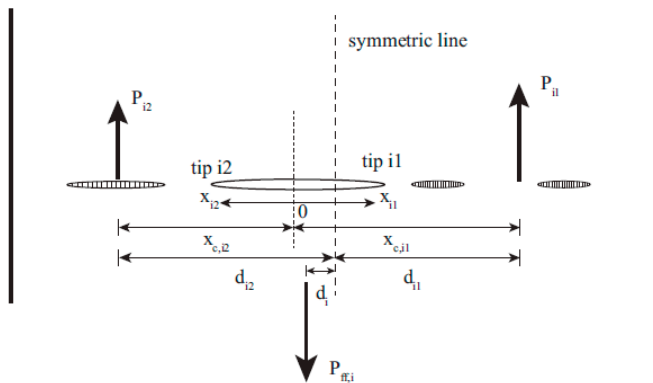
### 4.1 Multiple-Site Damage crack growth behaviour in Fibre Metal Laminate structures

Wandong Wang, Calvin Rans, Rinze Benedictus, TU Delft

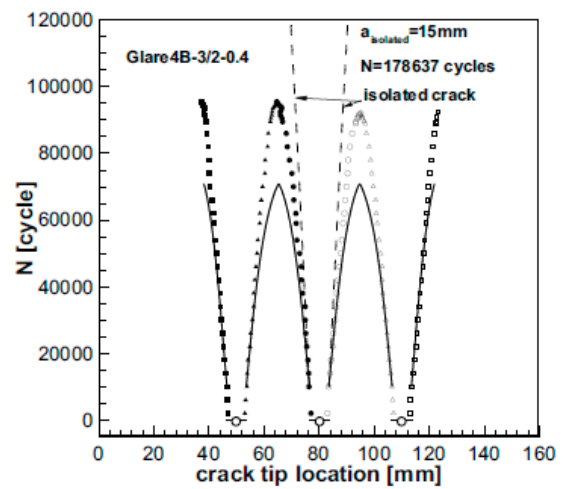
The present research deals with the crack growth behaviour in FMLs containing multiple cracks. Compared to the case of an isolated crack in an FML, multiple cracks further undermine the laminate stiffness, resulting in more deformation of the laminate. Precise analysis and calculation of the associated deformation and stress states for this sophisticated phenomenon is intricate. To simplify the problem, other adjacent cracks are idealized as “negative stiffeners” so that the reductions in the geometric stiffness due to the cracks can be modelled in a simplified way when calculating the stress states of a single crack. The methodology involves invoking a strain compatibility condition between the layers of an FML containing multiple cracks, allowing the increase in stress due to adjacent cracks to be determined for a single crack location. This analysis can be repeated to permit the determination of crack tip stress intensity factors for multiple cracks. The proposed approach was found to be computationally efficient and produce acceptable and conservative predictions for crack growth behaviour in FMLs under an MSD scenario.



(a) Illustration of stress distributions



(b) Illustration of balanced equivalent loads



(c) Comparison of MSD test results with predictions for MSD and a single isolated crack

Figure 12: Illustration of stress distribution and concept of balanced loads (left) and comparison between experimental results and predictions (right).

More information is provided in ref. [8].

## 4.2 Assessment of the fatigue and quasi-static damage directionality in Fibre Metal Laminates

Mayank Gupta, René Alderliesten, Rinze Benedictus, TU Delft

Theories in literature for the behaviour of fatigue crack growth and quasi-static crack growth all assume the application of axial loading in the principal material directions, i.e. in the direction of fibre orientations. Loading FMLs in directions other than the material direction will not only affect the rate of damage growth, but also its directionality. The direction in which cracks propagate under fatigue and quasi-static loading is observed to be affected by the mode mix near the crack tip in the metal layers. Hence, the maximum tangential stress (MTS) theory for predicting crack paths has been identified to be most suitable for describing the damage directionality in FMLs.

The mode mix at the crack tip is governed by two aspects: the orthotropy of the laminate, which in case of unbalance with the loading axis, imposes additional shear loading while introducing axial loading to the panel, and the off-axis orientation of the fibres bridging the fatigue crack, see Figure 13. The first aspect can be determined from the laminate's angularity and directionality.

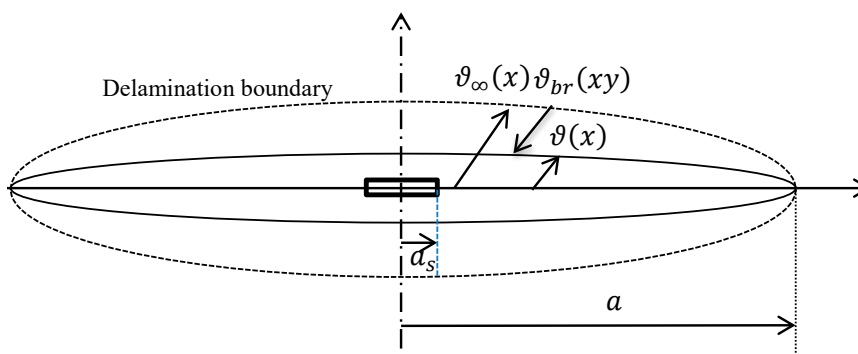


Figure 13: Illustration of the crack opening due to far field loading, and the opening restraint imposed by the off-axis bridging fibres.

In case of quasi-static loading, representing the residual strength condition, the absence of fibre bridging does not limit the mode mix at the crack tip to be influenced by laminate orthotropy only. Development of plasticity will change the compliance of the panel and as result changes the effective orthotropy, resulting in substantially larger angles with respect to the pane transverse to loading, see Figure 14.

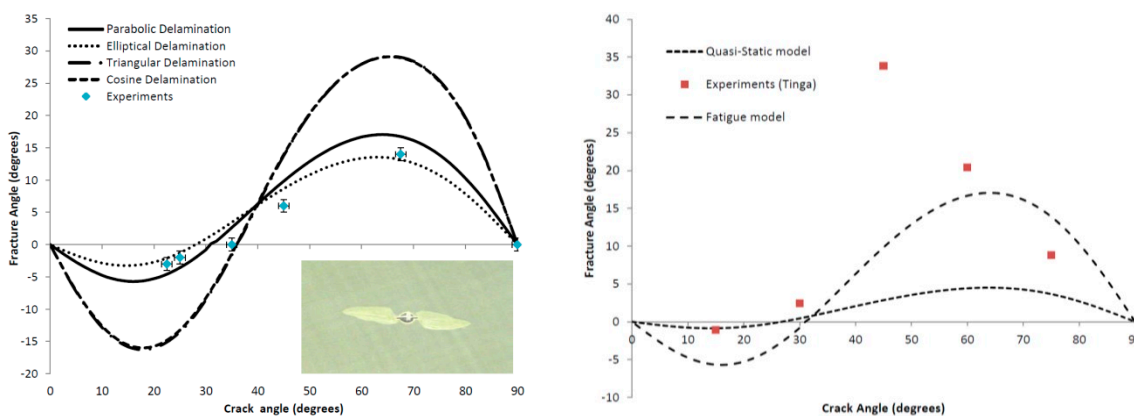


Figure 14: (a) Comparison between predicted and experimentally measured fracture angles in fatigue crack growth, and (b) similar comparison for quasi-static crack growth.

The theory has been validated to experimental evidence obtained during the research and obtained previously within the GLARE development program for the Airbus A380. The developed theory is based on linear elastic fracture mechanics which appears well applicable to fatigue crack growth, but insufficient to capture the mode mix at the crack tip in quasi-static crack growth as result of significant plasticity.

More information is provided in ref. [9].

### 4.3 Thermal strains in heated Fibre Metal Laminates

*Bernhard Müller, Jos Sinke, Andrei Anisimov, Roger Groves, TU Delft*

Current trends in aircraft design go towards smart materials and structures including the use of multi-purpose materials. Fibre Metal Laminates (FML) with embedded electrical heater elements in leading edges of aircraft used for anti- or de-icing follow those trends. The laminated structure of FMLs such as GLARE with layers of different materials leads to anisotropic material characteristics. The anisotropic structure raises questions concerning possible effects on the material characteristics when frequently heated by embedded heater elements and cooled by flight conditions. In order to investigate those possible effects on FMLs, knowledge about the thermal strains and stresses is important. Furthermore, non-destructive techniques are likely to be a future requirement to detect defective heater elements and delaminations at heated leading edges. Thus, this research uses a shearography (speckle pattern shearing interferometry) instrument (Figure 15, a) in order to investigate the surface strain components of manufactured GLARE specimens during thermal loading with the embedded heater elements. The manufactured specimens included various heater shapes and designs as the reference heater element without artificial delaminations or imperfections due to connection techniques, heater elements with different connecting techniques (overlap, soldered, spot welded), one heater element with artificial delaminations and one s-shaped heater element.

Parallel to the experiments, numerical analyses were conducted in order to investigate the strain-stress state due to thermal loading with embedded heater elements. The results of both, the strain measurement with the shearography instrument and the numerical analyses were analysed and compared (Figure 15, b and c). The numerical results showed how the embedded heater element affected the residual stress-strain state and the stresses due to thermal loading.

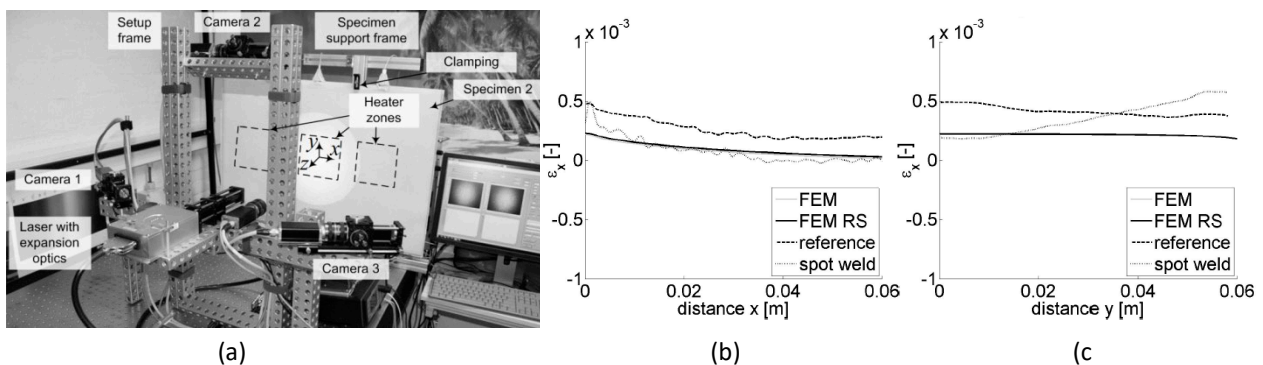


Figure 15: (a) Developed multicomponent shearography experimental setup used to measure the surface strain components, (b,c) comparison of the experimentally measured and numerically modelled values of the surface strain component  $\epsilon_x$ .

It was shown that using shearography to measure displacement gradients and interpret them as strain components during the thermal loading of GLARE leads to reasonable results. The numerical model was validated with the

experimentally measured surface strain components. Further the model was used to predict the stress-strain and temperature distributions through the thickness of the material which is not possible to do with experimental inspection techniques.

More information is provided in ref. [10].

## 4.4 Assessing the contribution of the process zone ahead of the mode II delamination tip in CFRP laminates

*Lucas Amaral, René Alderliesten, TU Delft*

The use of laminated composite materials in primary structures is still limited by the occurrence of in-service delaminations. Considering that interlaminar shear is one of the predominant loads experienced by composite structures, understanding the damage mechanisms involved in mode II delaminations is crucial for the development of a damage tolerance philosophy. Therefore, it was examined whether the energy dissipated in the process zone ahead of the crack tip should be accounted for when assessing fatigue delaminations caused by in-plane shear.

ENF quasi-static and fatigue tests were performed and the results show that damage propagates ahead of the crack tip in a process zone. Acoustic Emission (AE) was used to verify that the process zone dissipates a significant amount of energy which should be accounted for when characterizing mode II delamination growth, as shown in Figure 16. The extent of the process zone in an ENF specimen cannot be measured by the means of visual observations made from the side of the specimen. Therefore, the definition of a crack tip is not recommended in mode II delamination studies. In fact, the concept of damage in composites under mode II loading has to be revisited.

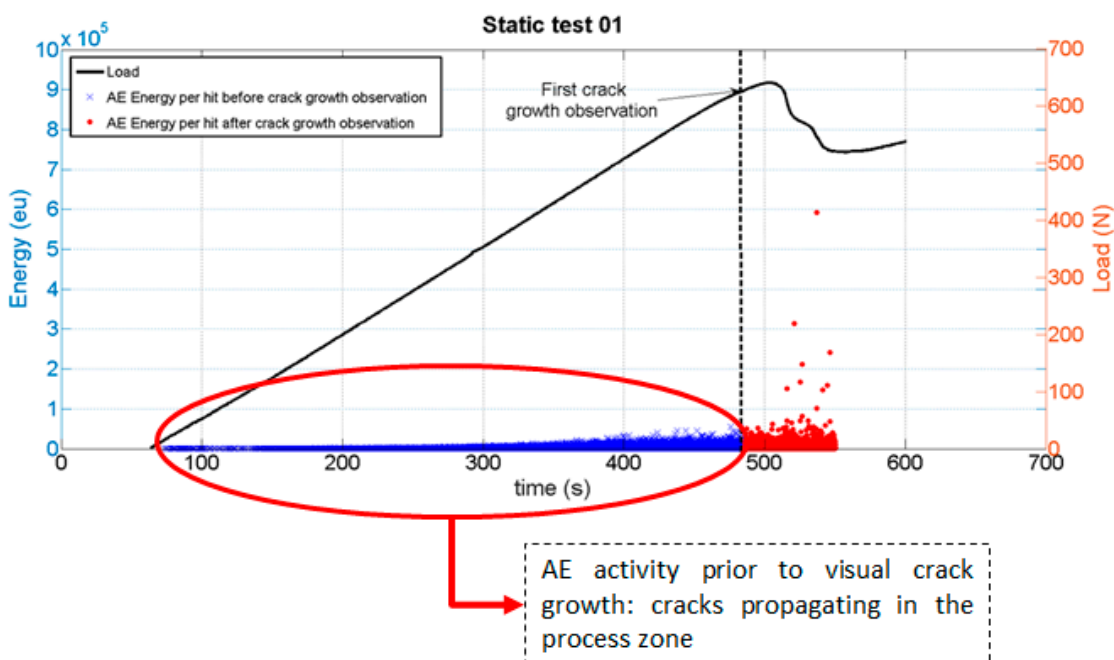


Figure 16: Static test monitored by AE.

Following previous work available in literature, further research is performed in this area with the objective to understand the formation of damage ahead of the crack tip in mode II conditions. In this study, PVC foam is loaded in shear, in an attempt to simulate the behaviour of the resin layer in-between fibres in a composite under delamination growth. The results, shown in Figure 17, illustrate that the concept of a crack is not appropriate for mode II delaminations, because energy is dissipated in a process zone ahead of the crack tip.

### PVC foam loaded in shear – Fatigue Test – Where is the crack tip??

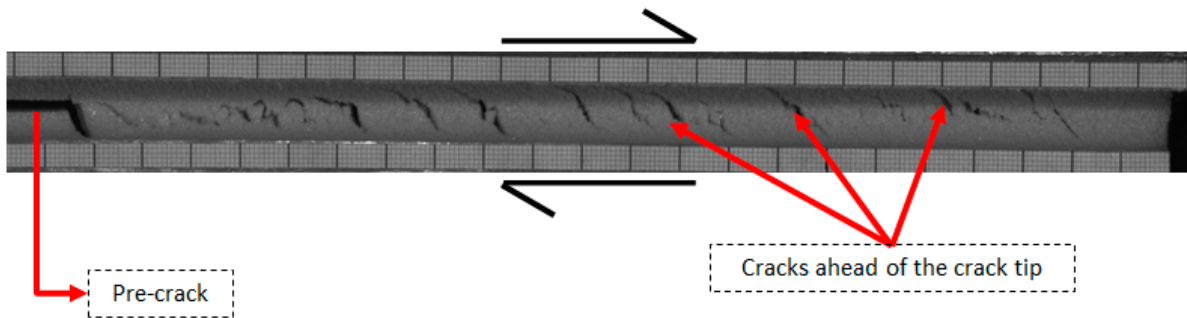


Figure 17: PVC foam shear.

## 5 Prognostics & Risk Analysis

### 5.1 Real-time fatigue life prognostics of composite structures using stochastic modelling and SHM data

*Dimitrios Zarouchas and Nick Eleftheroglou, TU Delft*

The field of prognostics of the remaining useful life (RUL) of composite structures, based on in-situ experimental data, is of great interest, towards a condition-based maintenance process, for several engineering applications i.e. aerospace, wind energy, automotive. This field of research is very promising as it can provide, during the in-service life of the structure, real-time estimation of the RUL and build the confidence of the operator for reliable decision-making. This study uses a data-driven prognostic methodology, which does not make any assumption about the damage mechanics involved during the life of the composite structure. The non-homogeneous hidden state Markov model (NHHSMM) was utilized in order to simulate the process of damage accumulation under fatigue loading. The NHHSMM enables multi-state degradation modeling, assuming that the damage accumulates gradually and increases during service. The model is characterized by an initialization and training procedure. The initial topology is obtained by defining the following elements: the number of possible hidden or discrete degradation states, the transition diagram that defines the allowed transitions between the hidden states, the probability density function which characterizes the sojourn time at each hidden state, the degradation histories (observations) and the observation quantization since the data's domain is continuous.

A fatigue experimental campaign of seven open-hole CFRP specimens was performed in order to test the validity of the proposed prognostic methodology. The specimens, with  $[0, \pm 45, 90]_2$ s lay-up, were subjected to fatigue loading with maximum amplitude 90% of their static tensile strength,  $R=0$  and  $f=10$  Hz.

Two in-situ experimental techniques, digital image correlation (DIC) and acoustic emission (AE) were used in order to monitor the strain evolution and record the signal activity due to the fatigue damage process. The strain and AE degradation histories of the seven open-hole specimens are presented in Figure 18. AE was continuously recording the signal activity until the failure of the specimens while DIC was periodically capturing pictures.

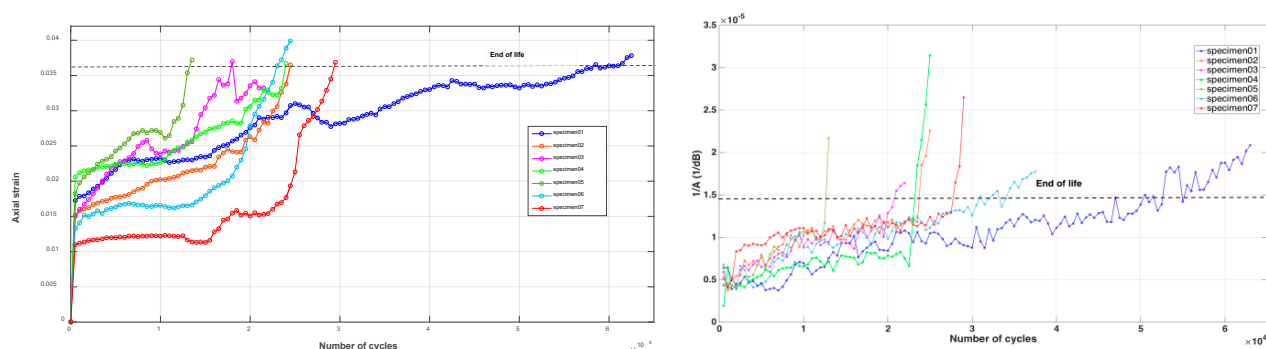


*Figure 18: Axial strain (a) and Amplitude accumulation (b) degradation histories.*

Figure 19a and Figure 19b present not only the estimations for the mean, median RUL but also provide a 90% confidence interval of RUL for specimen03 based on strain and acoustic emission data respectively. The choice of this specimen was random, similar results were obtained for the rest specimens.

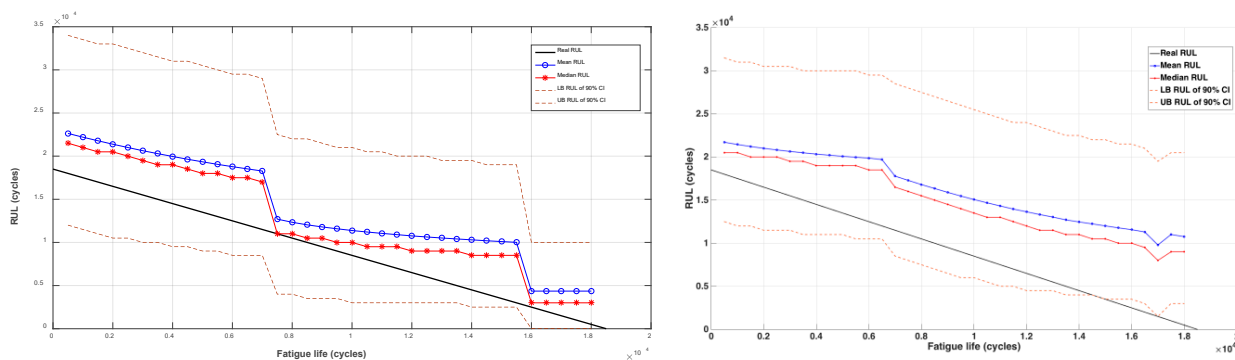


Figure 19: Mean and median estimations with 90% confidence intervals for (a) strain data and (b) AE data.

It was observed that strain data provided more reliable predictions for the RUL in comparison to AE data. This is partly due to the fact that strain data is straightforwardly derived from the DIC method while for AE, extensive signal processing is needed in order to identify data that describes the damage accumulation process.

Currently, the research group works on data fusion strategies in order to provide an optimum data set, derived from both in-situ techniques, as input to the probabilistic mathematic model.

## 5.2 Probabilistic life prediction model for welded structures

Frank Grooteman, NLR

Within the European project LIFEMOD, a probabilistic life prediction model has been developed by NLR for welded IN718 components that contain defects from which cracks can initiate and grow up to failure. Considerable scatter is present in the life from component to component, due to scatter in defect size, material properties and loads, where in general the scatter in defect size causes most of the scatter in the life of the component. A probabilistic living model, taking into account variability due to initial defect size, material properties and loads, and any other important scatter sources, was expected to improve the component design life, compared to the current deterministic design approach.

The developed probabilistic living model is very flexible and can take into account sources of scatter for all parameters in the deterministic model. The deterministic model consists of a crack growth tool (NASGRO) and a fatigue analysis tool (Cragro++, NLR-proprietary) and can be easily extended with other tools. The probabilistic part is formed by a generic probabilistic tool RAP++ (Reliability Analysis Program), which has been developed by NLR over the past 20 years.

The probabilistic living model allows for a generic set-up of the analysis problem without the need of source code modifications. Typically the analysis consists of: 1) definition of the deterministic analysis, 2) using the deterministic model in a probabilistic sensitivity analysis using approximate distributions that model the variability in the various model parameters to determine the most important scatter sources, 3) a reliability analysis to determine the probability of failure. The probabilistic model was enhanced with a failure model for multiple defects of different type.

During LIFEMOD an extensive experimental program was performed on IN718 dog-bone specimens with various dimensions manufactured by GKN Sweden. The geometries of the specimens were line-scanned and the part of the welds CT scanned by Carl-Zeiss Sweden. The line-scans were used to feed a parametric finite element model to

compute the residual stress field present after welding, due to bending and offset, for each individual specimen. With the CT scans internal defects could be located and quantified. High-cycle fatigue tests were performed by SP Technical Research Institute Sweden and the fracture surfaces were examined afterwards by Sulzer Netherlands. This experimental database subsequently can be applied to generate part of the probabilistic input data and improve the current deterministic design approach. The LIFEMOD project was coordinated by Swerea KIMAB Sweden who performed a batch of creep fatigue tests on similar IN718 specimens.

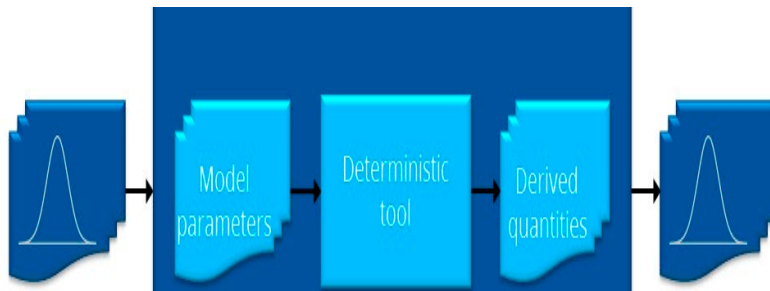


Figure 20: Schematised probabilistic analysis with RAP++.



Figure 21: Dog-bone HCF specimen.

## 5.3 Thermal loads in a business jet horizontal stabilizer

Jan Waleson, Fokker Aerostructures

The horizontal stabilizer of a large cabin business jet was designed by Fokker and included composite-to-metal hybrid structure that produced significant thermally-induced loads. The design of the metal structure for Fatigue and Damage Tolerance (FDT) and the thermal tests for correlation of the strains with FEM were a considerable effort. Successful FAA/EASA certification was achieved with an “analysis supported by test” approach using a full-scale mechanical fatigue test together with a finite element model (FEM) for thermal loads, which was validated by a separate full-scale thermal test. The metallic inspection intervals were affected by thermal loads based on the analysis. The structure was not susceptible to Widespread Fatigue Damage as meant in ref. [14]. Compliance was shown with 14 CFR25.571 up to and including Amendment 25-132.

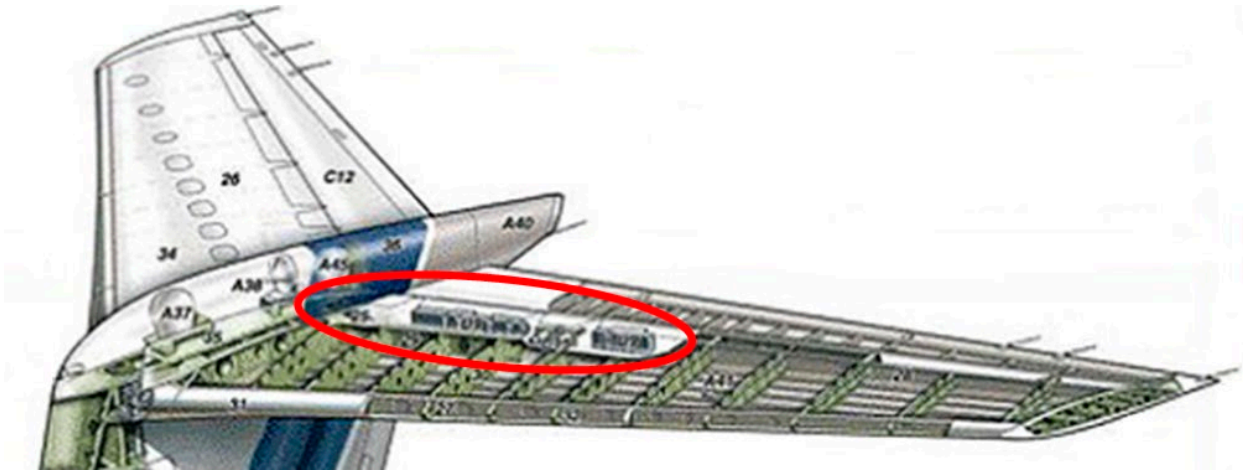


Figure 22: Location of left-hand center beam, which is joined to the pivot fitting beam at the root.

### Structure sensitive to thermal loads

The hybrid primary structure consists of:

- CFRP skins, front and rear beams (spars);
- A corrosion resistant steel (CRES) pivot fitting beam, aluminium center beams attached to the pivot fitting beam, and aluminium ribs – see Figure 22.

The long combined load path of the center beams attached to the pivot fitting beam attracts significant thermal loads.

### Temperature range for static loads

The structural temperature range that was considered for static load cases was  $-55^{\circ}\text{C} \rightarrow +80^{\circ}\text{C}$  ( $-67^{\circ}\text{F} \rightarrow +176^{\circ}\text{F}$ ). The lower bound covers air temperatures down to  $-80^{\circ}\text{C}$  ( $-112^{\circ}\text{F}$ ) by taking credit for the aerodynamic heating at  $M = 0.85$ . In a similar project in which Fokker designed the horizontal stabilizer, a 2D thermal model was used to analyse tropical conditions at noon for a dark horizontal surface. The upper skin temperature on the ground was shown to drop to  $+80^{\circ}\text{C}$  ( $+176^{\circ}\text{F}$ ) in the first flight segment with relevant loads due to forced convection. Since the selection of static load cases provided by the OEM was based only upon mechanical loads (not operating conditions), Fokker combined all load cases with both temperature extremes as a conservative approach.

### Temperature range for fatigue loads in design phase

The following structural temperatures for FDT were considered during the design phase:

- Based upon experience with previous projects, as a conservative approach, a ground temperature of  $+50^{\circ}\text{C}$  ( $+122^{\circ}\text{F}$ ) was assumed;
- Temperatures in the flight segments were based upon the International Standard Atmosphere, while the effect of aerodynamic heating was computed using the equation for adiabatic wall temperature [15], [16]:

$$\frac{T_{\text{total}}}{T_0} = 1 + \frac{\gamma - 1}{2} e M_a^2$$

Good conductivity was assumed from the exterior surface through the CFRP skin and aluminum ribs and center beam, and hence, little lag of structural temperature compared to skin temperature, which was later confirmed by flight tests. In the design phase, the critical mechanical load of the approach segment (see Figure 23) was combined with the low temperature of a previous flight segment, since the CRES pivot fitting beam has thermal inertia and the skin is locally shielded from the airflow by the vertical tail plane and the fairing on top of the horizontal stabilizer.

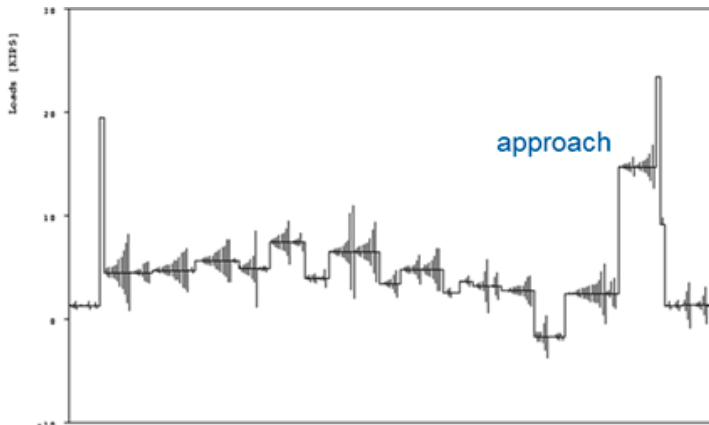


Figure 23: Typical flight spectrum with high mechanical load on pivot fitting beam upper cap in the approach segment.

### OEM ground and flight temperature measurements for FDT in certification phase

In the certification phase, the ground conditions of a hot day (ISA + 17°C / ISA + 31°F plus solar heating) were simulated by an array of high powered lights and structural temperatures were measured on a test aircraft. Structural temperatures were also measured on typical flights. It was confirmed that the ribs and center beam show relatively fast response to the temperature at the skin surface. Static air temperatures in flight appeared to be somewhat lower than those of the International Standard Atmosphere and were incorporated in the OEM structural temperature model. A significant temperature lag due to thermal inertia and the local shielding from the airflow by the vertical tail plane and top fairing was measured on the beam web of the pivot fitting, to which the structural temperature model was correlated. Figure 24 shows how well the OEM structural temperature model for analysis correlates also for the pivot fitting beam with its thermal inertia and with the local shielding from the airflow.

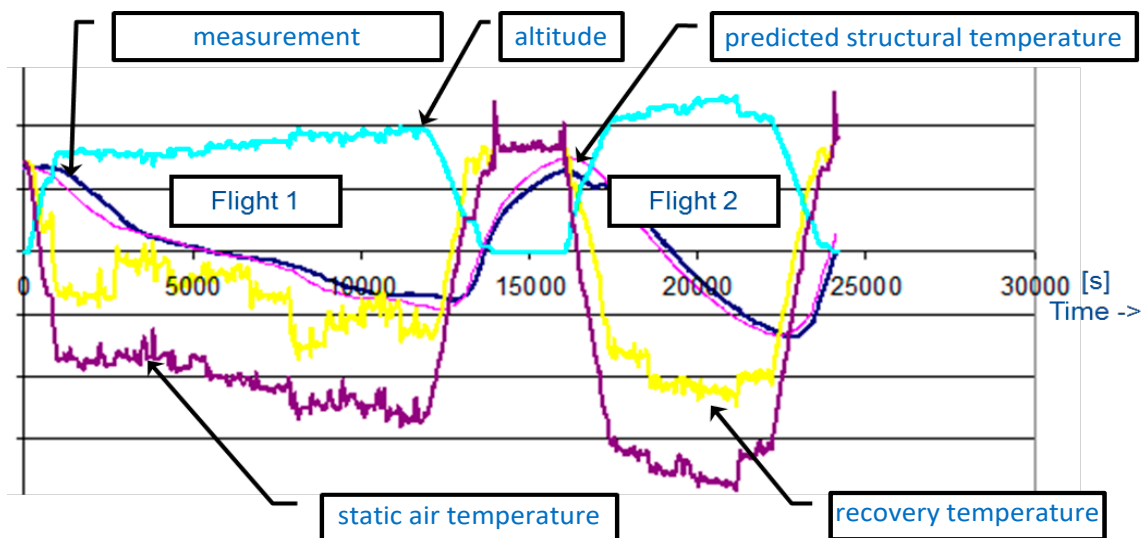


Figure 24: Excellent correlation of structural temperature predicted by OEM structural temperature model for analysis with measured temperature for the pivot fitting beam with its thermal inertia and with the local shielding from the airflow.

### Modelling joints in fine-grid FEM model

A fine-grid FEM model was used for analysis of the composite structure and mainly the FDT analysis of the metal structure. Combinations of mechanical and thermal loads were run. Joints were modelled per bolt, initially with infinite stiffness of the joining element, which is considered a conservative approach - see Figure 25. Later, a joint stiffness according to Huth [17] was incorporated into the FEM model.

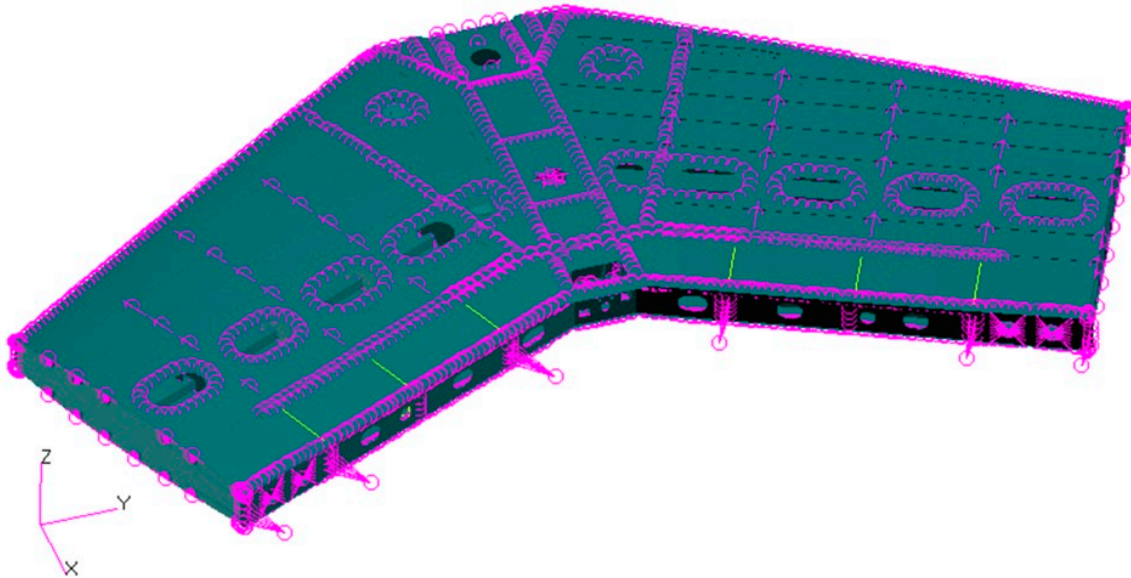


Figure 25: Fine-grid FEM model with joints modeled per bolt.

**Correlation of thermal loads in FEM and tests**

Strains were measured in several full-scale thermal tests to validate the computed thermal loads:

- On the instrumented horizontal stabilizer static and FDT component test article in an autoclave at Fokker at higher temperatures – see Figure 26;
- On the OEM test aircraft at Eglin Air Force Base at both lower and higher temperatures.

These tests validated the FEM modelling of the thermal loads, especially of joints, by correlation of the strains.



Figure 26: Thermal test on the instrumented horizontal stabilizer static and FDT component test article in an autoclave at Fokker.

### Thermal loads and mechanical loads in spectrum

The contribution of the thermal loads was significant for this structure. Figure 27 shows an example of the spectrum of a long flight with and without the thermal loads at the aluminum center beam upper cap.

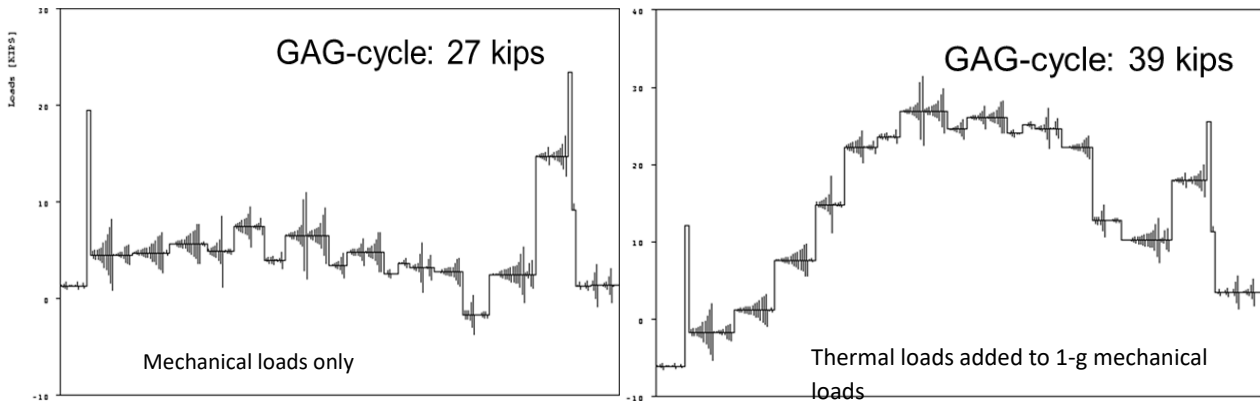


Figure 27: The loads at the aluminum center beam upper cap in a long flight (left = mechanical loads only; right = the thermal loads added to the 1-g mechanical loads).

### Structure covered by analysis (supported by test)

It was challenging to include the thermal loads in the room-temperature full-scale tests, since using mechanical overloads does not accurately represent the induced thermal loading. The following metal structure and composite structure attached to it are especially affected by thermal loads, which, therefore, were covered by analysis, supported by test:

- The long metal load path of pivot fitting beam and center beam – see Figure 28;
- The aluminum ribs (especially with respect to the static analysis of joints and girders and fatigue);
- The joints of the aluminum leading edge.

Based upon the demonstrated correlation of thermal strains in FEM and full-scale thermal-only testing the static analysis was done with a factor of safety  $j = 1$  for thermal loads.

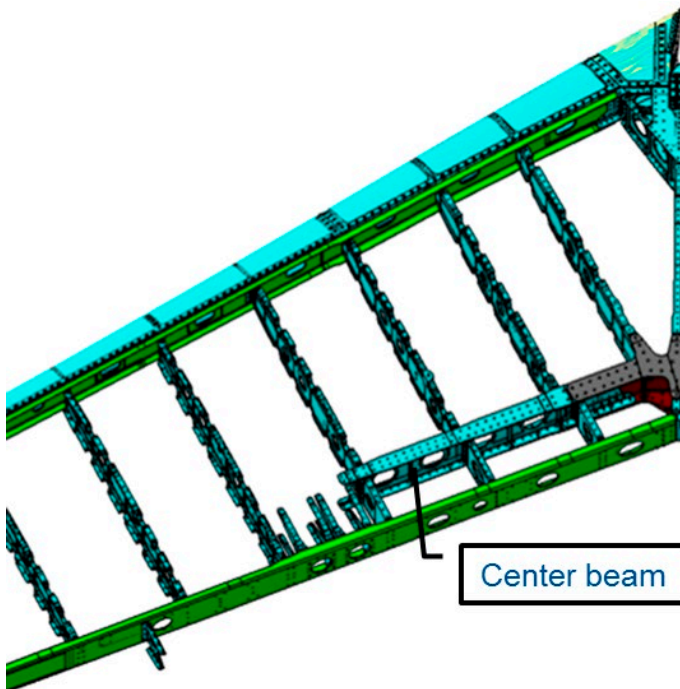


Figure 28: The long metal load path of the center beams joined to the pivot fitting beam.

**Compensating for missing thermal loads in DT test**

The critical inspection interval of a multi-element metal joint with directed inspection was affected by the thermal loads. The analysis was to be validated by test. However, the metal structure was tested in a dedicated FDT airframe test, in which thermal loads were not covered. Therefore, in general, thermal loads were covered by analysis, validated by full-scale thermal-only testing. Since the horizontal stabilizer component test for the composite portion had a Load Enhancement Factor LEF=1.15, it appeared that the predicted fatigue damage using analysis almost enveloped the predicted fatigue damage including the effect of thermal stresses. The test period had to be slightly elongated only. Thus, this horizontal stabilizer component test for the composite portion was used to validate the inspection interval of the metal joint.

## 6 Non-Destructive Evaluation

### 6.1 Near-infrared optical coherence tomography for inspection of fibre composites

Ping Liu, Liaojun Yao, Roger Groves, TU Delft

Optical coherence tomography (OCT) is a non-invasive imaging method, which allows the reconstruction of 3D depth-resolved images with high resolution. Originally developed for biomedical diagnostics, nowadays it also shows a high potential for applications in the field of non-destructive testing (NDT). This work [11] describes the investigation of fibre composites using a customized OCT system. It can perform as an inline inspection tool to monitor the crack growth and reconstruct the crack surfaces in glass fibre composites [12]. It can also work as a profilometer which is able to rebuild 3D crack profiles within carbon fibre composites, as shown in Figure 29. These types of information provided by OCT allow researchers to easily access delamination related parameters, e.g. crack lengths during a tensile test, and to observe delamination propagation modes, e.g. crack jump in different layup composites. OCT can greatly improve the facilities for delamination research and could contribute more in the near future with its development in faster and deeper scanning.

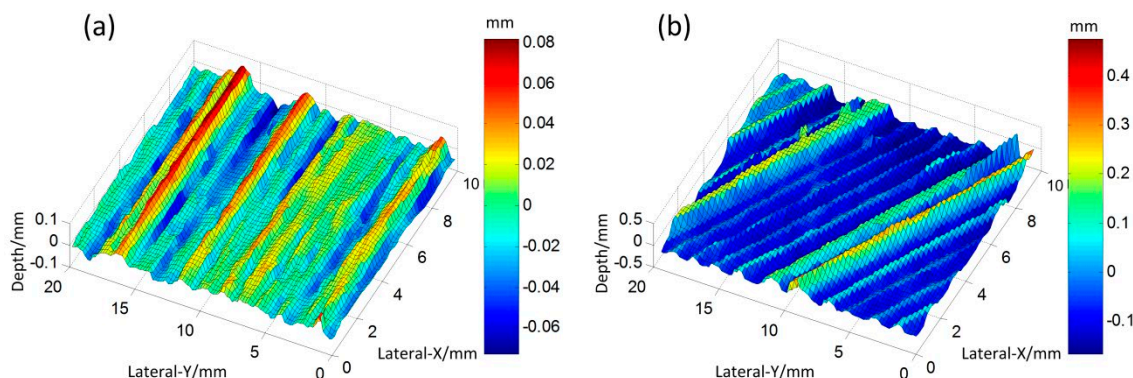


Figure 29: 3D crack profiles of carbon fibre composites. The 0 and 45° colour lines indicate the fibre orientation. The colour bars indicate the surface height.

### 6.2 Evaluating delamination growth in composites under dynamic loading using infrared thermography

J.K. Narayana Swamy<sup>a,b</sup>, F. Lahuerta<sup>a</sup>, A.G. Anisimov<sup>b</sup>, R.P.L. Nijssen<sup>a</sup>, R.M. Groves<sup>b</sup>,  
<sup>a</sup>Knowledge Centre WMC, <sup>b</sup>TU Delft

This research involved the development of a method for the quantitative analysis of a delamination area under dynamic loading using thermography [13]. To demonstrate this method, a coupon was developed with double shear configuration and an initial delamination consisting of a PTFE insert. The coupon was tested under fatigue loading and an infrared (IR) camera was used to monitor the thermal response and delamination growth of the coupon during the loading (Figure 30a). The data from the thermal camera (Figure 30b) was processed in 2 steps. Firstly a fast Fourier transform (FFT) was used to transform the raw data from time domain to frequency domain (Figure 30c). In the second step, FFT thermographs were further processed using an image segmentation algorithm. The thermal plots were segmented to separate the delaminated and un-delaminated areas (Figure 30d). The delaminated area was

obtained at each cycle by computing the number of pixels in it. Further the size of the estimated delaminated area was plotted against the cycles to failure. The strain energy was computed with the help of force and displacement data from the test machine. Such signals allowed computing the fatigue propagation curves and understanding the fatigue behaviour of the test samples.

The delamination growth estimated with the developed method was compared with the results obtained inspecting the coupon with a visible camera. The comparison was done continuously during the fatigue testing. The difference in the delamination area estimated the by the IR camera and the visible camera was less than 10%.

The results of the developed method were promising since the experimentally evaluated delamination growth curve was in good agreement with a power law and visual inspection methods. The developed method can produce quantifiable measurements and its output can be used as a starting point to study delamination growth experimentally and computationally. Moreover, it was shown that the developed method could be extended to different coupons types that could not be quantitatively analysed using the conventional inspection techniques.

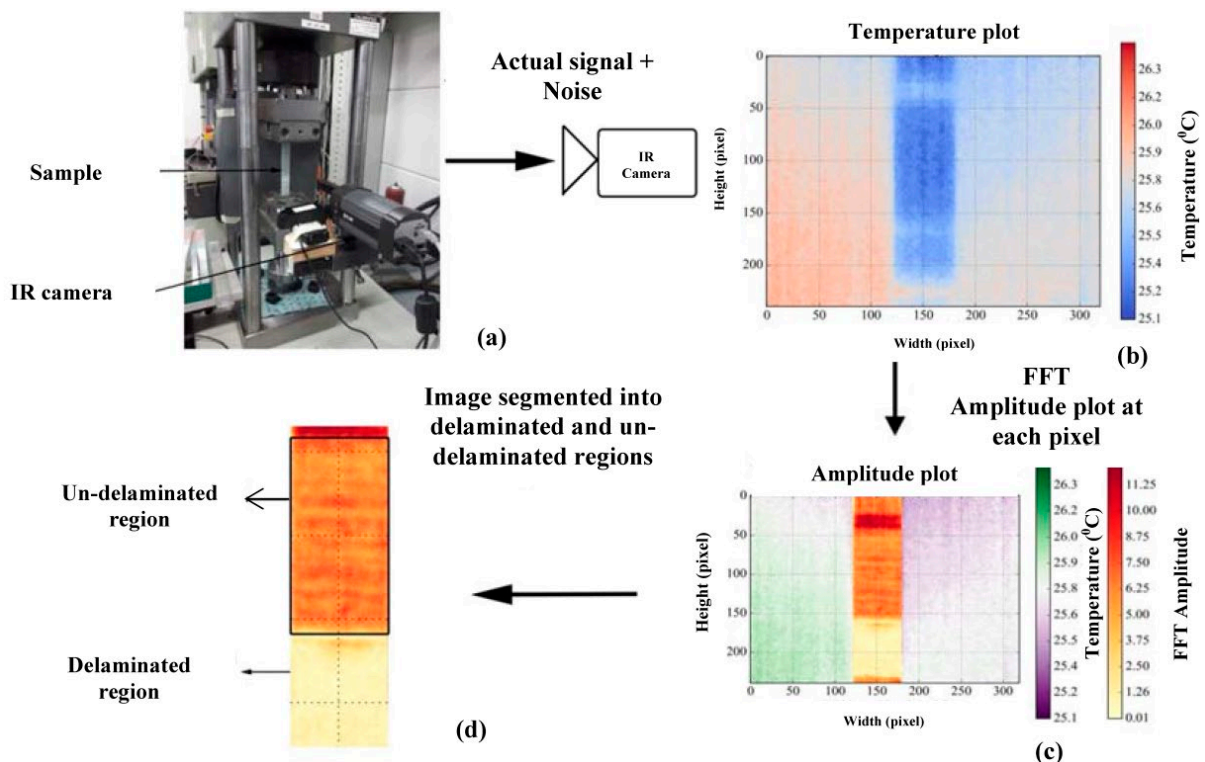


Figure 30: Block diagram of the processing algorithm: (a) the sample in the test frame, (b) temperature plots obtained from the IR camera, (c) FFT amplitude plot and (d) processed image with segmented delaminated and un-delaminated area.

## 6.3 Analysis of chemical degradation of thermally cycled glass-fibre composites using hyperspectral imaging

V. M. Papadakis, B. Müller, M. Hagenbeek, J. Sinke, R. M. Groves, TU Delft

The application of glass-fibre composites in light-weight structures is growing. Although mechanical characterization of those structures is commonly performed in testing, chemical changes of materials under stresses have not yet been well documented. In the present work coupon tests and Hyperspectral Imaging (HSI) have been used to categorise

possible chemical changes of glass-fibre reinforced polymers (GFRP) which are currently used in the aircraft industry. HSI is a hybrid technique that combines spectroscopy with imaging. It is able to detect chemical degradation of surfaces and has already been successfully applied in a wide range of fields including astronomy, remote sensing, cultural heritage and medical sciences. GFRP specimens were exposed to two different thermal loading conditions. One thermal loading condition was a continuous thermal exposure at 120°C for 24h, 48 h and 96h, i.e. ageing at a constant temperature. The other thermal loading condition was thermal cycling with three different number of cycles (4000, 8000, 12000) and two temperature ranges (0°C to 120°C and -25°C to 95°C). The effects of both conditions were measured using both HSI and interlaminar shear (ILSS) tests. No significant changes of the physical properties of the thermally cycled GFRP specimens were detected using interlaminar shear strength tests and optical microscopy. However, when using HSI differences of the surface conditions were detected. The results showed that the different thermal loading conditions could be successfully clustered in different colours, using the HSI linear unmixing technique. Each different thermal loading condition showed a different chemical degradation level on its surface which was indicated using different colours, shown in Figure 31.

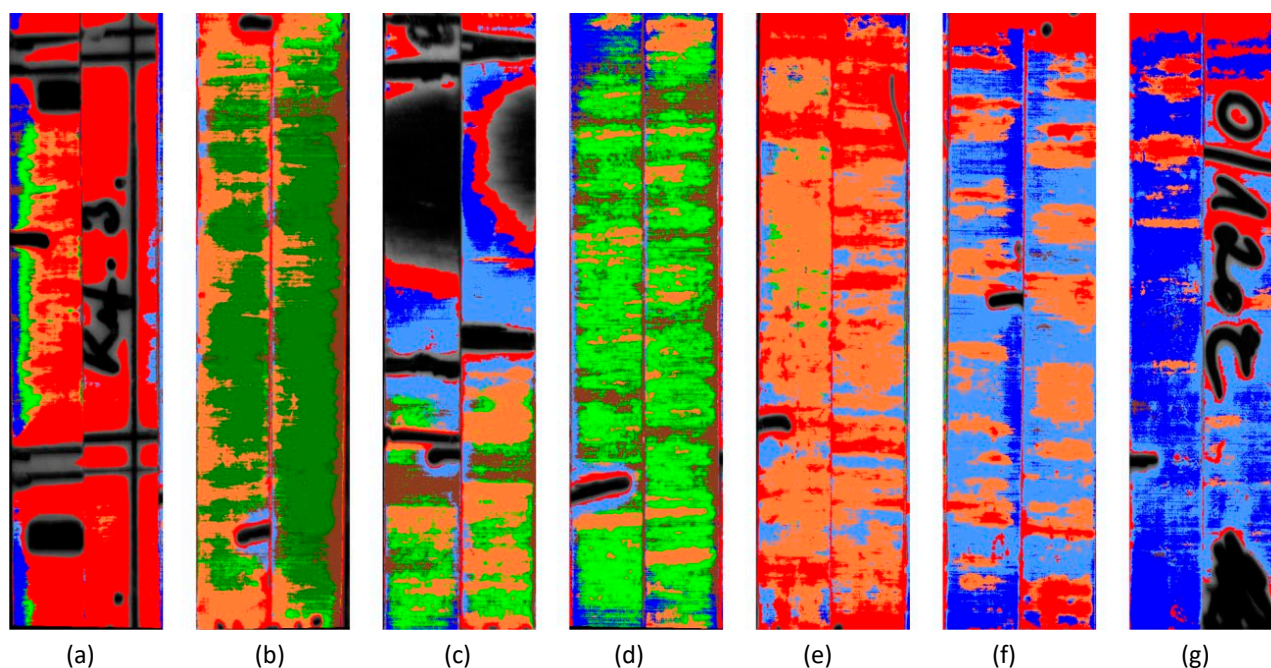


Figure 31: Hyperspectral images of the thermal cycled specimens: (a) Reference, (b) -25/+95 4000 cycles, (c) -25/+95 8000 cycles, (d) -25/+95 12000 cycles, (e) 96 h 0/+120 4000 cycles, (f) 96 h 0/+120 8000 cycles and (g) 96 h 0/+120 12000 cycles. Note that black and grey areas are not categorized with the algorithm.

This work has been presented at SPIE Smart Structures NDE, Las Vegas, in March 2016.

## 6.4 In-service ultrasonic detection of impact damage in thick-walled composites

Jaap Heida, Jacco Platenkamp, Arnoud Bosch, NLR

This work involved an investigation into the applicability of the ultrasonic testing method (UT) for the in-service detection of impact damage in thick-walled composite structures. Visual inspection remains the primary in-service inspection method for composites, including the detection of impact damage in thick-walled composite structures, but

UT is recommended in case of suspected damage during visual inspection. The investigation has shown that suitable UT techniques include phased array (UT-PA) and a UT array camera:

- UT-PA equipment gives impact damage detection results which are comparable to the results obtained with conventional UT C-scan base-line inspection, apart from small sizing differences. All impact damages are best detectable with the PEFR scans (pulse-echo flaw reflection), both in the C-scan and in the cross-sectional scans (B-scans).
- The UT array camera that was considered has less penetration depth than UT-PA equipment, and the impact damage areas are not well marked off (sizing is not reliable), but relevant impact damage areas are clearly detectable in the different scan views of the camera (A-scan, B-scans and amplitude/TOF C-scans). A basic assumption, herewith, is that if damage has occurred in thick composite structure after impact then it will always include sub-surface damage directly underneath the impact location (depth range about 0 – 5 mm).
- The UT array camera that was considered has a limited field of view (31 x 31 mm) but a special stitching mode easily provides C-scan presentation of larger damage areas. An evaluation with the RTM calibration specimen of Figure 32 showed that the detection of a 6 mm diameter flat-bottomed hole at a depth of about 9 mm seems to be a rough estimate for the sensitivity of inspection of the camera at larger depth.

The following guidelines are given for in-service verification of suspected impact damage during visual inspection of thick-walled composites:

- UT array camera as fast and cost-effective method to verify if relevant damage is indeed present at the suspected location;
- UT phased array inspection to fully characterise the damage (size, depth) for repair purposes.

The implementation of these UT techniques could depend on the maintenance level, for example a UT array camera available for all field level maintenance and phased array UT equipment only for depot level maintenance.



Figure 32: The RTM trailing arm of Fokker Landing Gear that was used as a calibration specimen in the investigation.

## 6.5 In-service inspection of water ingress in composite honeycomb structures

*Jaap Heida, Jacco Platenkamp, Arnoud Bosch, NLR*

This work involved an investigation into the applicability of the thermography and ultrasonic inspection methods for the in-service detection of water ingress in composite honeycomb structures. The investigation showed that for both inspection methods the applicability is dependent on the extent and distribution of the water in the honeycomb cells. Fully filled cells are well detectable but partly filled cells, on the other hand, are considered not reliably detectable. For those cells it is imperative that the entrapped water must be in contact with the skin laminate that is being inspected.

Of the two inspection methods, thermography is best suited for the in-service detection of water ingress in composite honeycomb structures. The good detectability of water ingress by thermography is caused by the relatively high specific heat capacity of water relative to composite material. As a result, after an imposed heat pulse surfaces in contact with trapped water appear to be cooler (and are hence well visible) in the thermographic image than the surrounding dry area. A special advantage of thermography is that it is a truly non-contact inspection technique and capable of inspecting surface areas up to 1 m<sup>2</sup> with a single exposure technique. For practical in-service applications commercial equipment is available. It is remarked that the applicability of thermography is dependent on the specific excitation technique (e.g. transient and Lockin). It is recommended to further investigate the influence of different skin thickness and the presence of excess adhesive or sealant.

Manual ultrasonic phased array inspection is considered less suitable for the in-service detection of water regarding its sensitivity of inspection and the observation that a proper time-of-flight scan is not possible. However, especially for fully filled cells, a standard reflection C-scan is then still possible. Further, manual UT pulse-echo inspection with a single UT transducer is not practical for the inspection of large areas but it can be used to quickly verify any suspect areas for water ingress with fully filled honeycomb cells, almost irrespective of the test frequency of the transducer.

All results considered it is concluded that ultrasonic inspection will remain the main method for the in-service detection of most significant defects in composite materials such as impact damage, delaminations and disbonds. However, for the specific requirement of the detection of water ingress in honeycomb structure, thermography is better suited, especially for the global and fast inspection of large surface areas.

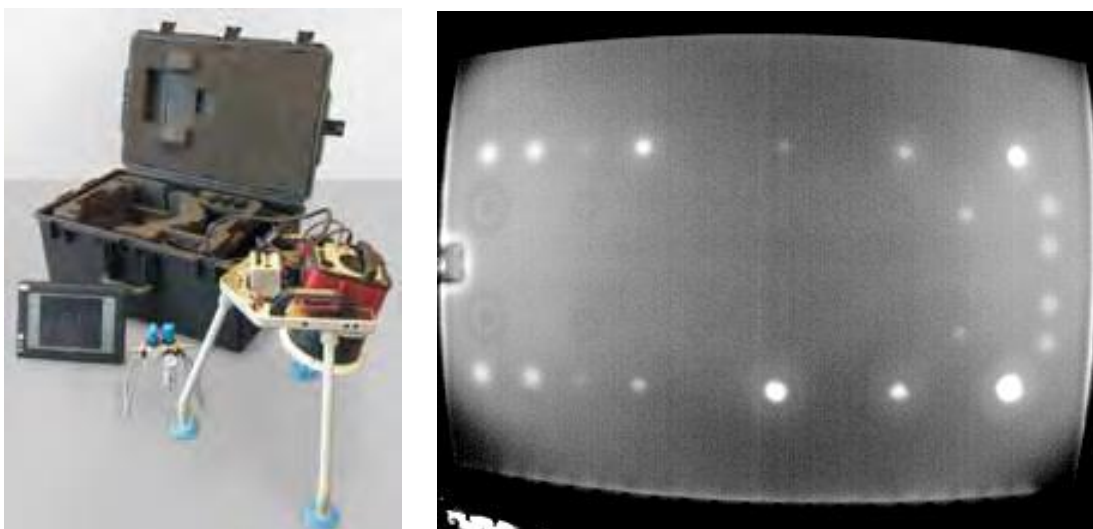


*Figure 33: Thermography inspection of a honeycomb panel with water ingress.*

## 7 Structural Health & Usage Monitoring

### 7.1 Fielding a Structural Health Monitoring system on legacy military aircraft: a business perspective

*Marcel Bos, NLR*

An important trend in the sustainment of military aircraft is the transition from preventative maintenance to condition based maintenance (CBM). For CBM, it is essential that the actual system condition can be measured and that the measured condition can be reliably extrapolated to a convenient moment in the future in order to facilitate the planning process while maintaining flight safety. Much research effort is currently being put in the development of technologies that enable CBM, including structural health monitoring (SHM) systems. Good progress has already been made in sensors, sensor networks, data acquisition, models and algorithms, data fusion/mining techniques, etc. However, the transition of these technologies into service is very slow. This is because business cases are difficult to define and the certification of SHM systems is very challenging.

In an attempt to break through this deadlock, a paper has been written that describes a possibility for fielding an SHM system on legacy military aircraft (such as the F-16) with a minimum amount of certification issues and with a good prospect of a positive return on investment – see ref. [20]. For appropriate areas in the airframe the application of SHM will reconcile the fail-safety and slow crack growth damage tolerance approaches that can be used for safeguarding the continuing airworthiness of these areas, combining the benefits of both approaches and eliminating the drawbacks.

The idea that is set forth in the paper only works for fail-safety managed damage tolerant aircraft structure as meant in USAF Structures Bulletin EN-SB-08-001. For such structure it is conceivable to install SHM sensors at the primary structural load path without relying on them for safety. The SHM system is then used for economic reasons only, to detect cracks in the primary structural area while they are still small and easy to repair. In case the SHM system fails to do so, safety is not jeopardized since the continuing airworthiness of the aircraft is still managed by means of fail-safety with visual inspections for large cracks. This means that certification of the SHM system will not be much of an issue, whereas the business case of potentially avoiding large and expensive repairs without the need for cumbersome NDI may be sufficiently worthwhile to justify the upfront investments in the development and installation of a suitable SHM system.

This idea may be rather trivial but the paper has been written in the hope of bridging the gap between the SHM community and the Structural Integrity community. The paper therefore provides a basic explanation of how damage tolerance works. Demonstrating SHM technology on flying aircraft will increase the TRL of the demonstrated technology and the confidence in its reliability and use needed for any military aircraft operator to accept it. Seizing this opportunity would be an evolutionary step towards more challenging applications.

## 7.2 Modal Strain Energy based Structural Health Monitoring of rib stiffened composite panels

Jason Hwang<sup>a,b</sup>, Richard Loendersloot<sup>b</sup>, Tiedo Tinga<sup>b</sup>, <sup>a</sup>NLR, <sup>b</sup>University of Twente

Maintenance strategies in various fields of industry, including aerospace applications, are shifting from time-scheduled to condition based. SHM techniques can play an important role by providing detailed information about the integrity of the target structure, while reducing the inspection time. Relevant aerospace applications include the monitoring of impact damages on composite rib-stiffened panel structures. For this application various methods are available. The present study considered one of them, viz. an in-house developed Modal Strain Energy (MSE) Damage Index (DI).

### Test article

Two identical composite panels have been manufactured similarly to a concept evaluated within the European Clean Sky LOCOMACHS project. Automated fiber placement was used to manufacture integrated stiffening ribs with a height of over 30 mm by stacking various layers of a single thermoset tape on an uncured skin – see Figure 34.

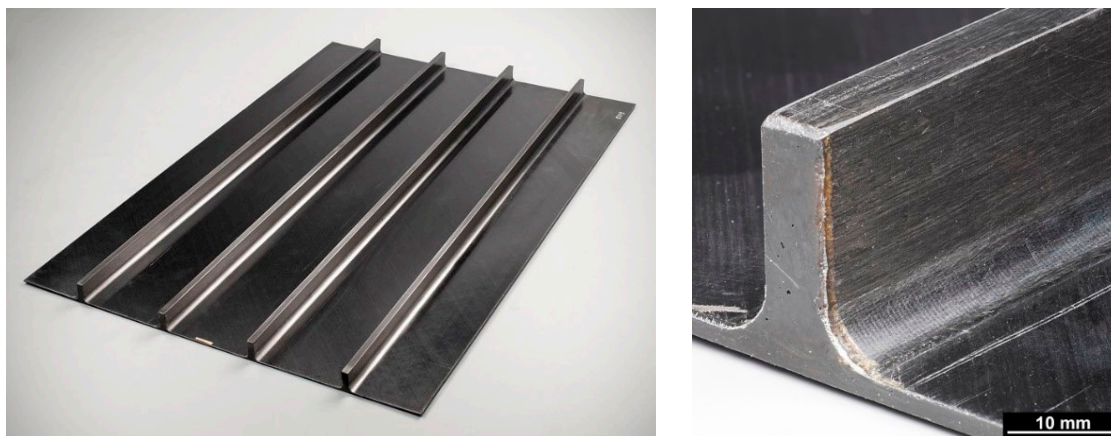


Figure 34: Rib stiffened co-cured panel (600 x 400 mm).

The table below presents a summary of the technical specification of the test panels.

Table 1: Specification of the test panels (all dimensions are given in mm).

Tow <sup>1)</sup> width	Length	Width	Layup	No. of plies	Remarks
6.35	600	400	[45/90/-45/0/45/90/-45/0] <sub>s</sub>	16	Skin
6.35	600	6.35	[0] <sub>177</sub>	177	4 ribs

1) Prepreg: CYCOM 5320-1FI/IM7

After fiber placement and curing, the panels were non-destructively evaluated via an ultrasonic C-scan inspection. The inspection revealed no major debonding, voids or defects in the skin and the skin-rib connections on the panels.

Both panels were subsequently subjected to a single impact load each. The panels were clamped on four edge sides, while stiffeners were kept unsupported such that a typical aircraft skin-stiffener condition is created. The impact was applied on the skin side, directly underneath stiffener 3 - see Figure 35 and Figure 36. The impact location on both panels was identical:  $x = 450$  mm and  $y = 250$  mm. The impact energy on the first panel was 18 J, while the second panel was impacted with 14 J. Non-destructive inspection with an ultrasonic probe revealed that both impacts had

caused a similar delamination at the skin stiffener connection. The impact loading on the outer skin side had caused no visible damage from the outside. However, the skin-stiffener connection was deteriorated significantly over a length of 150 mm.

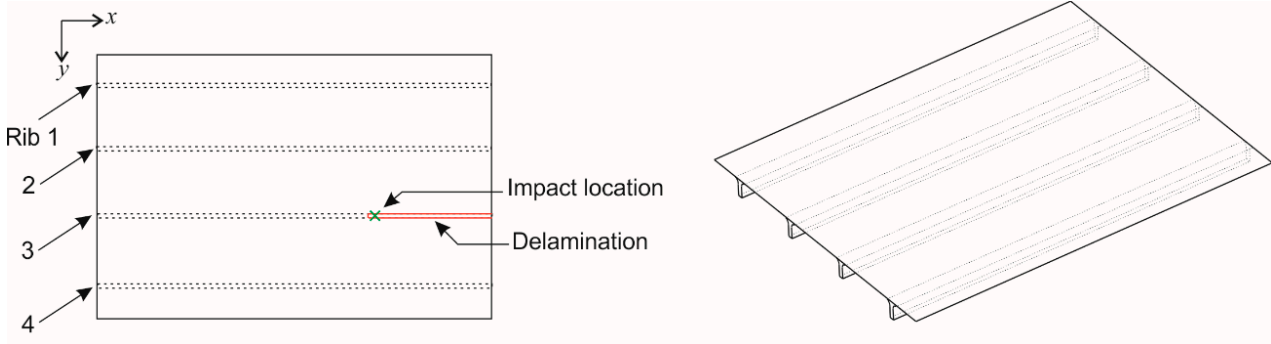


Figure 35: Schematic drawing of the rib-stiffened panel. Delamination size and location are similar to both panels.



Figure 36: Close up on the damage in the first panel.

## Methodology

Before and after impact loading, the natural frequencies and the Operational Deflection Shapes (ODS) of the test panels were extracted by using a Laser Doppler Vibrometer and an electro-mechanical shaker. The test panels were suspended with two rubber bands allowing for a free-free condition. The shaker was strategically placed such that all lower modes were sufficiently excited. The excitation consisted of series of 5 sine sweeps from 200 to 4000 Hz while the Laser Doppler Vibrometer measured the out-of-the-plane velocity with a measurement frequency of 48kHz. The measurement grid consisted of 23 x 11 points.

In this study, only one damage feature has been calculated, namely the MSE-DI (see ref. [18] for more details on this method). Since the bending stiffness of the panel in y-direction is dominant, the panel was modelled as a beam-like structure, allowing for a 1-D formulation of the modal strain energy equation in x-direction [19], following the considerations presented in this paper.

## Results

The natural frequencies and their corresponding operational deflection shapes have been extracted from both plates before and after the impact loading. For the normalized damage index calculation the amplitude normalized mode shape of the y-bending modes were used. Figure 37 presents the calculated MSE-DI for each of the plates.

It was concluded that the applied damages have been detected successfully on both panels, although the DI peaks appear at different locations, which implies an inaccurate damage localization. The highest normalized DI is found adjacent to the damaged area between stiffeners 2 and 3. However, a number of additional peaks in the MSE-DI appeared in the first panel, even while the impacts in both panels had been applied at the same location.

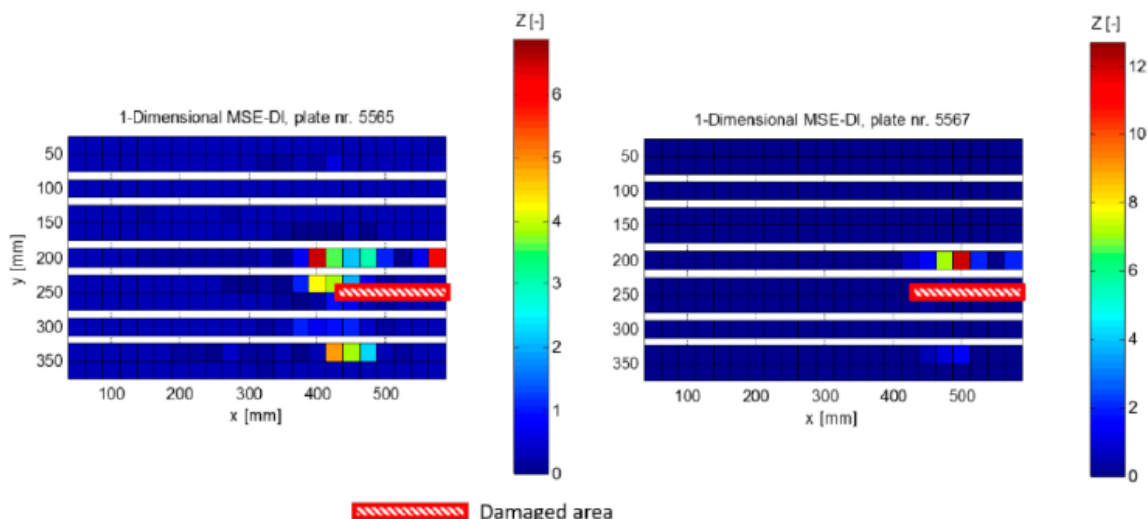


Figure 37: MSE-DI extracted from the dynamic responses of the two panels.

### Discussion

According to Ooijevaar et al. [19], bending modes in the y-direction are the most informative, but they were hard to measure, due to the high bending stiffness in that direction. This results in a limited accuracy of the damage localization, as this relies on an accurate estimate of the mode shapes. Deriving the second order of the displacement to determine the modal strain energy magnifies the localization inaccuracy. The considerations in ref. [19] apparently do not apply for this structure, indicating a relation between methods applied and the structure; a performance index should be able to reflect this. Future work will therefore include comparing various feature extraction methods to the performance of SHM techniques. The sensitivity to external factors will also be studied, to establish the robustness of methods in the performance indicator.

More information about this work is provided in ref. [21].

## 7.3 Experimental evaluation of vibration-based identification of damage in a composite aircraft structure with internally-mounted piezodiaphragm sensors

Jason Hwang<sup>a,b</sup>, Richard Loendersloot<sup>b</sup>, Tiedo Tinga<sup>b</sup>, <sup>a</sup>NLR, <sup>b</sup>University of Twente

The objective of this study was to develop and employ a piezo electric transducers based SHM strategy to a representative composite aerospace structure. Previous experiments with simple stiffened composite panels had demonstrated that delamination in a composite structure can be detected and localized by calculating and comparing the Modal Strain Energy (MSE) from vibration measurements on a pristine and damaged structure. In this study, a Carbon Fiber Reinforced Plastic (CFRP) aileron with a complex and representative aircraft geometry was considered with 19 internally-mounted piezo diaphragms, divided over two rows on and next to a stringer that was subjected to an impact load – see Figure 38. The sensor diameter was 5 mm. The structure was excited by an electro-mechanical shaker inducing a 50 to 1000 Hz sine sweep. The measured signals were used to compute an MSE damage indicator.

This study has shown the feasibility and limitations of a vibration-based modal-domain SHM strategy with an internally mounted sensing system. The piezodiaphragms were able to measure vibrational dynamics of the structure prior to and after the impact loading. Moreover, the mode shapes extracted from the measurement were successfully

employed to derive a Modal Strain Energy Damage Index (MSE-DI) that enabled to detect the presence of a damage. The localization of the damage was partly successful: One row of sensors indicated the presence of the damage accurately while the prediction of the second row was approximately 30mm off.

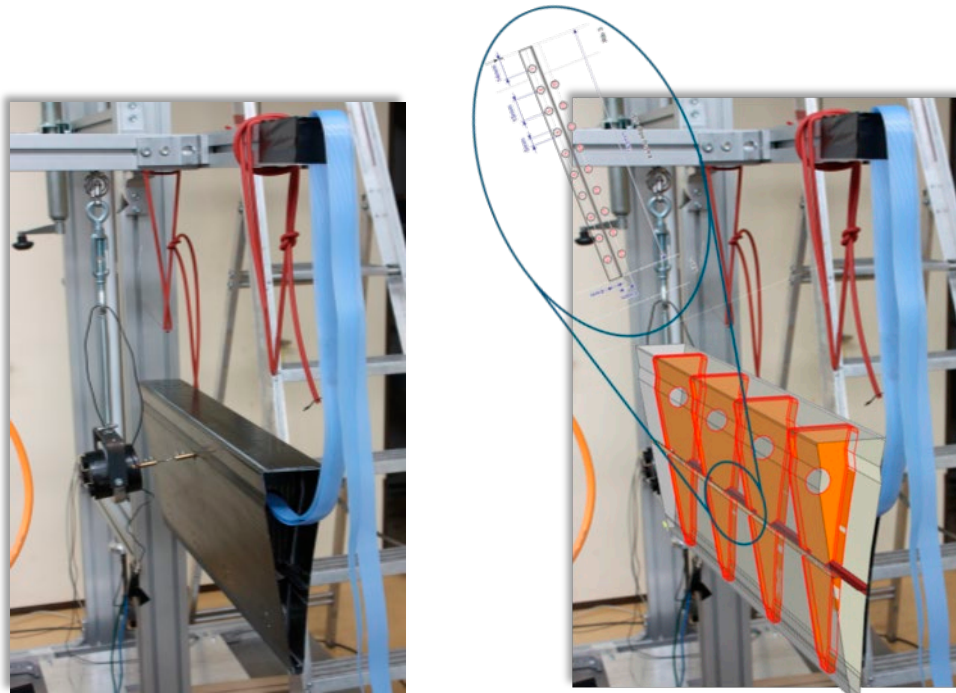


Figure 38: The freely suspended aileron with the shaker in the test rig (left) and the corresponding FE model (right).

More information about this work is provided in ref. [22].

## 7.4 Individual tracking of RNLAf aircraft

*Various authors, NLR, RNLAf*

The Royal Netherlands Air Force (RNLAf) and NLR collaboratively keep track of the loads and usage of most aircraft types in the RNLAf inventory, viz. the F-16 Block 15, C-130H/H-30, NH90, AH-64D, ICH-47D and ICH-47F.

This is done on an individual basis (individual aircraft tracking, IAT) and involves the installation of data acquisition and recording equipment, the development of databases and processing software, the development of fatigue and/or corrosion damage indices, the collection and processing of loads and usage data and the reporting of the processed data to the RNLAf. The results are used to:

- keep track of the consumed fatigue life;
- assess the severity of specific missions and mission types;
- evaluate and possibly optimize the usage of the fleets;
- optimize Maintenance programs;
- assess/anticipate required structural modifications programs;
- provide the OEM with high-quality data in case of modification programs;
- rationalise decisions regarding tail number selection in the case of out-of-area deployment, fleet downsizing, decommissioning, etc.;
- develop load spectra for full-scale component testing;

- gain insight in the root causes of accidents and failures;
- enhance reliability analyses.

Details of these programs were already supplied in previous National Reviews – see refs. [23]-[25]. More information is provided in refs. [26]-[30].



Figure 39: RNLAF aircraft types that are routinely tracked.

## 7.5 Towards condition based maintenance of drive train components of aging military helicopters

Marcel Bos<sup>a</sup>, Anne Oldersma<sup>a</sup>, LtCol Jan Jongstra<sup>b</sup>, LtCol Eric-Jan Verheem<sup>b</sup>, <sup>a</sup>NLR, <sup>b</sup>RNLAF

Fatigue loads and usage monitoring programmes are in place for most of the aircraft and helicopter types in the inventory of the Royal Netherlands Air Force (RNLAF). These programmes are primarily focussed on the airframe and the engines. From a cost perspective it is useful, however, to expand these programmes and include other systems as well. Many components in the dynamic system of a helicopter are life limited and need to be retired at prescribed times that are usually based on flight hours. The replacement intervals are based on conservative loads and usage assumptions. Knowledge of the actual loads and usage will thus enable to postpone retirement, which potentially will entail significant cost savings.

Elaborating on the IAT program CHAMP, the Chinook Airframe Monitoring Programme [29], the RNLAF and NLR are now evaluating ways to monitor the loads and usage of the drive train and rotor components of the RNLAF ICH-47D/F fleet [31]. The objective is to enable the transition from calendar based maintenance to condition based maintenance for these components. This will entail significant certification issues and therefore, as a first step, two relatively simple drive train components have been selected for a demonstrator program, viz. the forward and aft synchronizing shaft assemblies or ‘sync shafts’ – see Figure 40. These shafts transmit the power from the engines to the rotors and their loading is governed by the engine torques, which are measured by magnetostrictive torque meters at the engine output shafts. The measured torques are displayed in the cockpit in terms of a percentage. They are also recorded in the CVFDR and available in the flight data set that is routinely collected in CHAMP.

A fatigue model has been developed for the most critical location in the sync shafts that was able to reproduce the OEM specified retirement lives of 8,582 flight hours and 7,976 flight hours for the RNLAF ICH-47D forward and aft sync shafts respectively. These Boeing estimated lives are based on a design usage of six extreme Ground-Air-Ground/ power cycles per flight hour, each defined by Boeing as ‘the cycle from flat pitch to maximum power and back to flat pitch’, and a scatter factor of 4.0.

The calibrated NLR model has subsequently been used to estimate the sync shaft lives for the actual RNLAF usage, based on a batch of 111 measured sorties (202 flight hours) and using a scatter factor of 4.0. The results are shown in Table 2. They indicate that component lives specified by Boeing are extremely conservative. When the monitored sorties are typical of RNLAF usage, there is no need to replace the forward and aft synchronising shaft assemblies

during the 10,000-flight hour service life of the helicopter. This illustrates that - potentially - considerable savings can be achieved through individual aircraft monitoring.

Table 2: Specified versus actual fatigue life of the RNLAf Chinook sync shafts.

	Fwd Sync Shaft Assy	Aft Sync Shaft Assy
OEM specified retirement life:	8,582 flight hours	7,976 flight hours
Estimated actual fatigue life (SF=4.0):	348,862 flight hours	62,606 flight hours
Ratio Actual/Specified:	40.7	7.8

It is noted that in the life calculations some assumptions had to be made with regard to the distribution of the engine torque over the forward and aft sync shafts. This depends on the location of the helicopter centre of gravity (CG). The data documented on Form F “Weight & Balance” are not routinely collected as yet, although the fuel consumption is written to the avionics bus and is recorded by the CVFDR. For now, it has been assumed that the CG is located at STA 331 (Centre Cargo Hook) for all sorties analysed. Although this is considered to be a reasonable assumption, it is necessary to include a calculation of the rotorcraft CG to better determine the distribution of power over both rotors if the sync shaft life calculations are to be used in a fleet life management programme.

It is also noted that the NLR model has been calibrated against a very limited set of data. The life prediction estimates should therefore be classified as preliminary until more validation data becomes available, in the form of fatigue test data. A fatigue test program is currently being developed by NLR to test the lives of eight sync shafts that have been provided by the RNLAf, under two different flight-by-flight load spectra. A ninth shaft will be used to provide material for a coupon test program to generate the basic S/N curves.

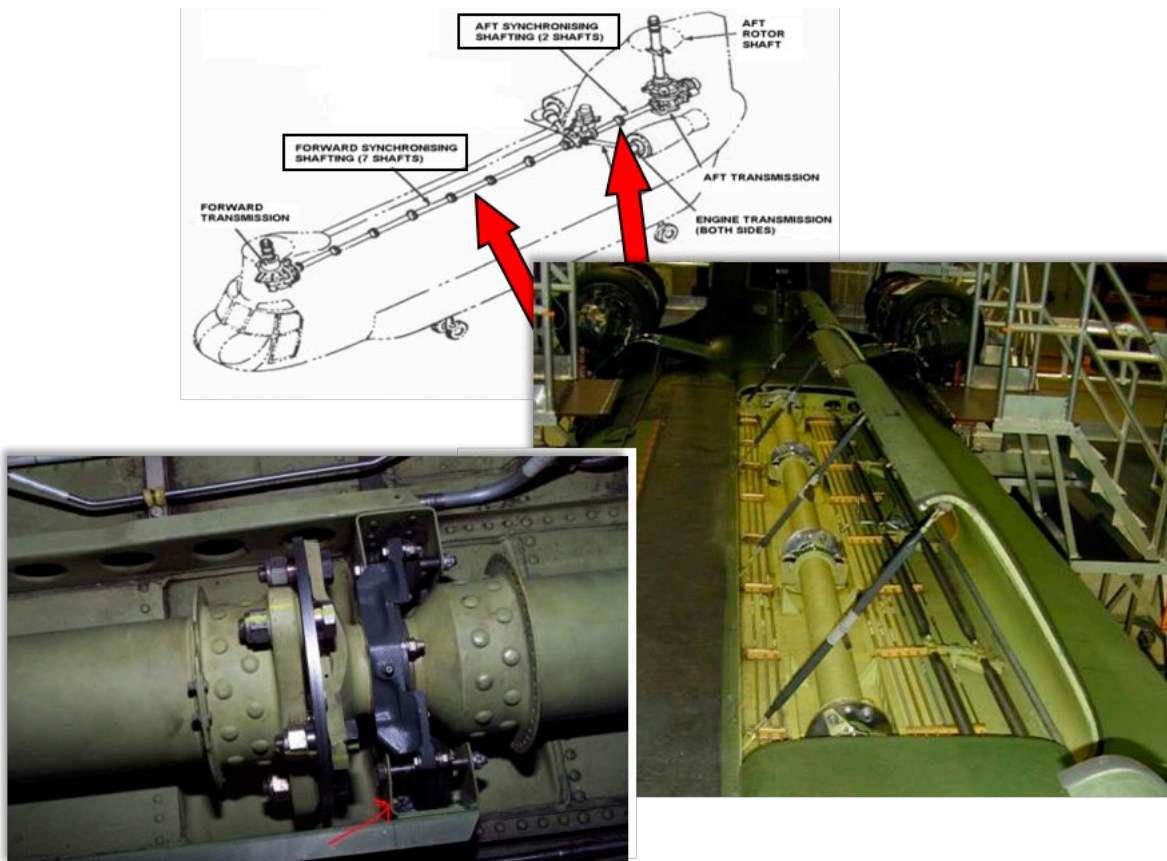


Figure 40: Chinook synchronizing shafts.

## 8 Advanced Testing

### 8.1 Advanced multi-axial testing of thermoplastic carbon composite laminates

*Jos Vankan<sup>a</sup>, Bas Tijs<sup>b</sup>, Jan de Jong<sup>a</sup>, Herman de Frel<sup>b</sup>, Niels Singh<sup>b</sup>, <sup>a</sup>NLR, <sup>b</sup>Fokker Aerostructures*

Composite laminates are being increasingly used in a wide variety of industrial applications, but there are difficulties in applying these materials in ways that exploit their full potential, in particular under multi-axial loading. The objective of the present study was to experimentally establish the biaxial failure data for composite laminates produced by Fokker Aerostructures based on the thermoplastic UD carbon reinforced material AS4D/PEKK-FC. For this purpose a test machine and accompanying cruciform specimens for in-plane biaxial failure tests have been developed – see Figure 41 and Figure 42. A coupon-level biaxial test program covering various biaxial load combinations in tension-tension, tension-compression and compression-compression has been successfully executed and biaxial failure values for the thermoplastic laminate have been determined. Besides the experimental biaxial test program, also finite element models and analyses have been used to predict the global outcomes of the biaxial tests and to interpret the test results. Both plain (unnotched) and open-hole (notched) specimens of the thermoplastic laminate have been tested. The biaxial failure data have been collected and further processed in biaxial failure criteria. From the experiments, the failure strains, stresses and loads have been determined and a failure envelope has been created for both plain and open-hole specimens. Good agreement was found between the theoretically predicted envelopes and the test data. From the findings for biaxial failure criteria from this study, it is expected that structural weight saving can be achieved in the design of multi-axially loaded composite parts as compared to the design with the previous uni-axially based failure criteria.

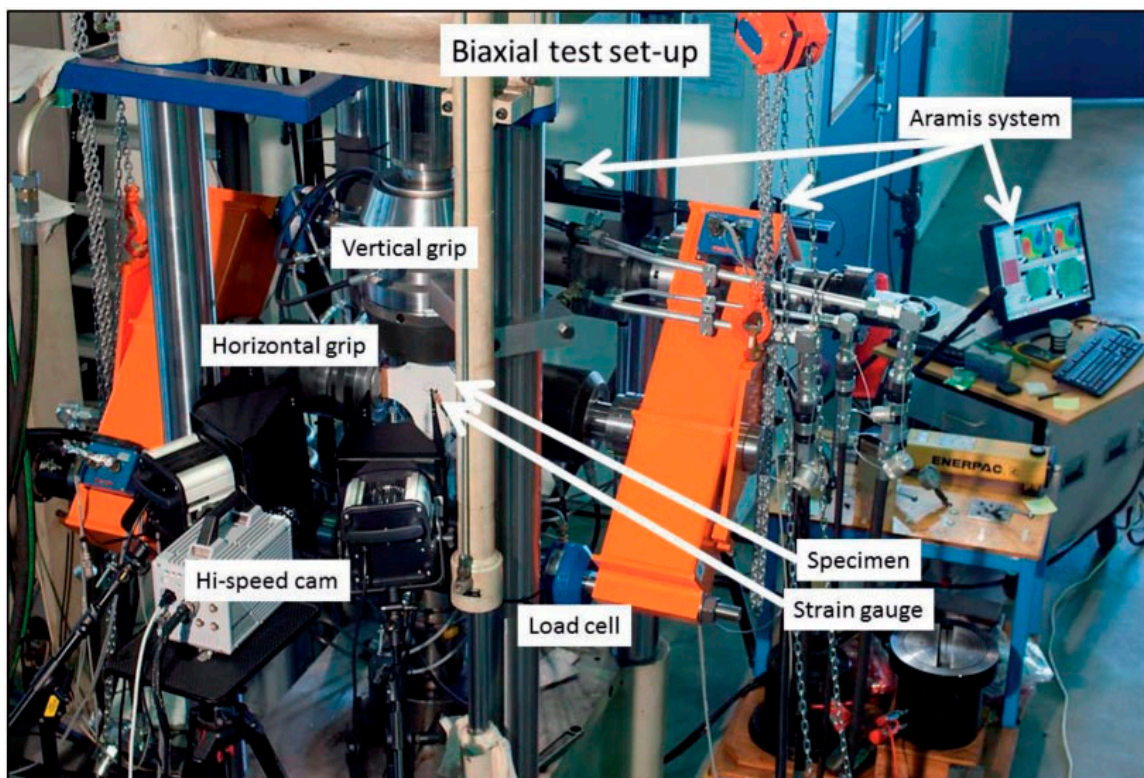


Figure 41: Biaxial test facility at NLR.

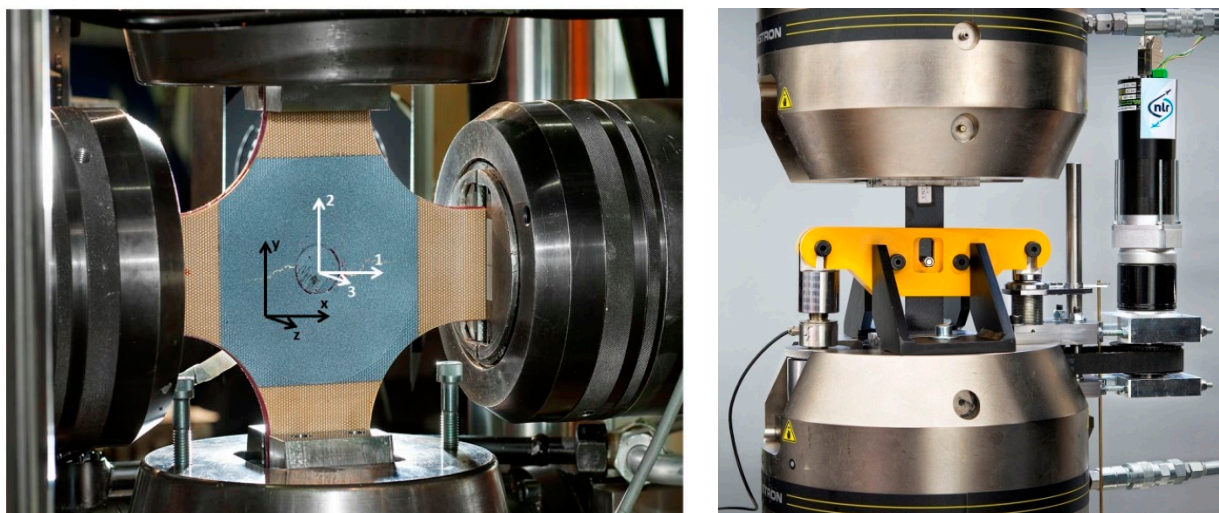


Figure 42: Multi-axial test set-ups at NLR for investigating the behaviour of thermoplastic carbon composite laminates: biaxial testing (left) and bearing-bypass testing (right).

More information about this work is provided in ref. [32].

## 8.2 Full-scale endurance testing of flap tracks at low temperatures

*Hotze Jongstra, Paul Arendsen, NLR*

Despite the continuous progress in simulation and modelling capabilities, testing is still of paramount importance to verify that airframe strength, durability and damage tolerance meet the requirements related to safety of flight. Testing already starts in the early design stage, when material allowables are to be established. Later on, testing needs to be done to validate structural design solutions and analysis methods. And, finally, full-scale tests on the complete aircraft or on major structural components are needed to generate inputs for the certification process. In all these tests, attention must be given to the effects of other parameters than loads as well, if these effects are expected to be (or cannot be excluded to be) of any significance. An important parameter in this respect is temperature. Material properties are known to change with temperature and predicting the temperature dependence of specific structural properties such as buckling behaviour and subsequent failure is not straightforward. Additionally, certifying the endurance (i.e. the wear and tear resistance) of a large mechanical subsystem under ambient test laboratory conditions may encounter serious objections from the authorities when actual service conditions include temperatures down to  $-55^{\circ}\text{C}$ .

Within this context NLR has developed both modular and specific cooling solutions for use in material and structures testing, based on the use of liquid nitrogen. Attention has been paid to affordability, maintainability, safety, scalability, accuracy and operating temperature range. The developed systems feature a high degree of autonomy, which makes them suitable for 24/7 applications, including certification tests at sub-assembly level. A current example is the certification test program of the Bombardier C-series flap tracks. These flap tracks are designed and manufactured by the Belgian company ASCO Industries. NLR has been contracted to conduct the full-scale static, endurance, fatigue and damage tolerance tests that are required by the certification authority, Transport Canada Civil Aviation.

The test setup consists of three independent modular rigs (one for each of the different tracks tested, see Figure 1 and Figure 43), each combined with an advanced electro-hydraulic actuation system. Electric rotary actuators are used to

dynamically control, through the original gear boxes, the positions of the carriages on the tracks. The loads on each flap track are distributed over its carriage and rear link through a so-called Load Introduction Device (LID) that essentially mimics the flap. Six independently controlled hydraulic actuators per test rig are connected to the LID. Three of the actuators are displacement controlled and serve to enforce the subtle and complicated out-of-plane (i.e. lateral) movement and orientation of the flap (represented by the LID in the test program) during extension and retraction. The other three actuators are force controlled and are used to apply the complex dynamic loads that are a function of the flap position. The position-dependent actuator loads have been computed using 6-DOF vector decomposition. They are provided to the Moog/FCS loads control system by means of a look-up table. In this way fatigue loading and endurance loading can be applied in a flight-by-flight manner and possible changes in the test specification can be handled in a very flexible way without having to redesign any hardware. Especially for the endurance test program this has turned out to be a major technical advantage.

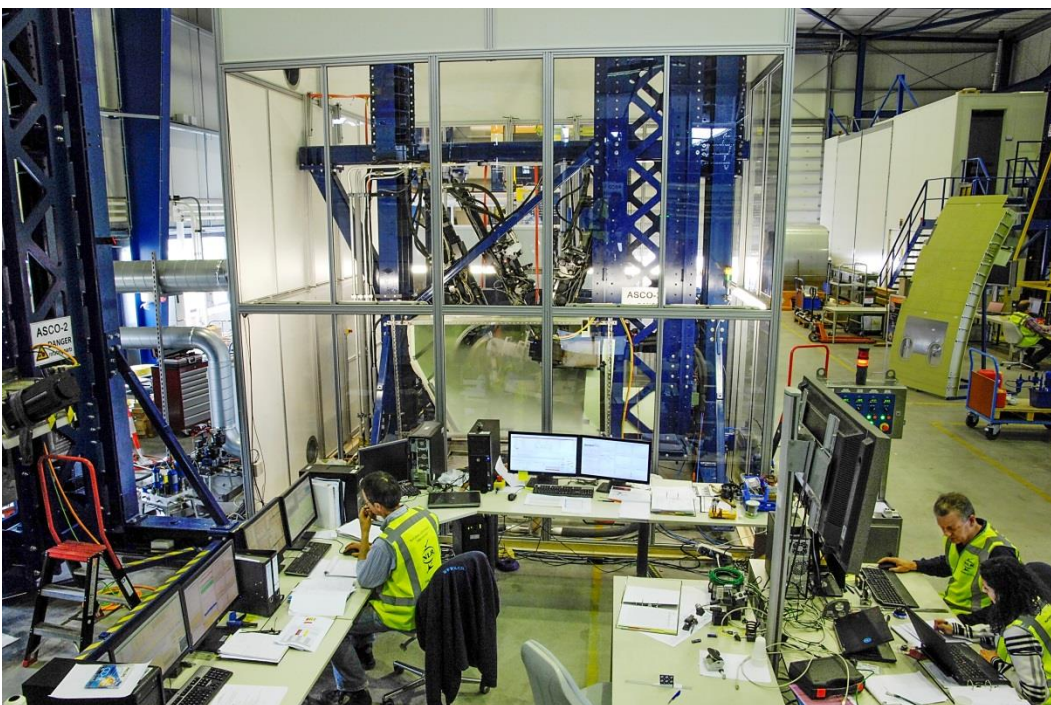


Figure 43: Overview of full scale flap track test setup at -55°C.

The endurance test program essentially is a full-scale system test in which the tracks are exposed to different contaminants (sand, dust, oil, ant-icing fluid, etc.) while operating at the true extension/retraction speed under representative flight loads. The endurance test specification called for a significant part to be performed at -55°C, for several weeks in a row, 24 hours around the clock.

The size and complexity of the test setup necessitated the use of an inner climate chamber, see Figure 44 (left), which roughly measures  $3 \times 1 \times 1 \text{ m}^3$ , and an outer cabinet of  $5 \times 5 \times 5 \text{ m}^3$ . The outer cabinet serves as a (i) buffer between the inner chamber and the ambient laboratory conditions, (ii) safety barrier to collect the nitrogen that inevitably leaks from the inner chamber due to the slots needed for the moving hydraulic actuators. Pre-filling the outer cabinet with dry nitrogen gas turned out to be instrumental in avoiding condensation and ice formation in the inner cabinet.

To prevent heat from the hydraulics being transferred to the cold test article, so-called thermal blocks are used to create a thermal barrier - see Figure 44 (right). These blocks act as heat sinks and insulate the cold test article from external heat sources. The thermal blocks are cooled down using special thermal pads and liquefied nitrogen. The

pads are capable of reaching  $-170^{\circ}\text{C}$  ( $-275^{\circ}\text{F}$ ) within minutes and have been developed in cooperation with experts from a local cryogenic engineering company.

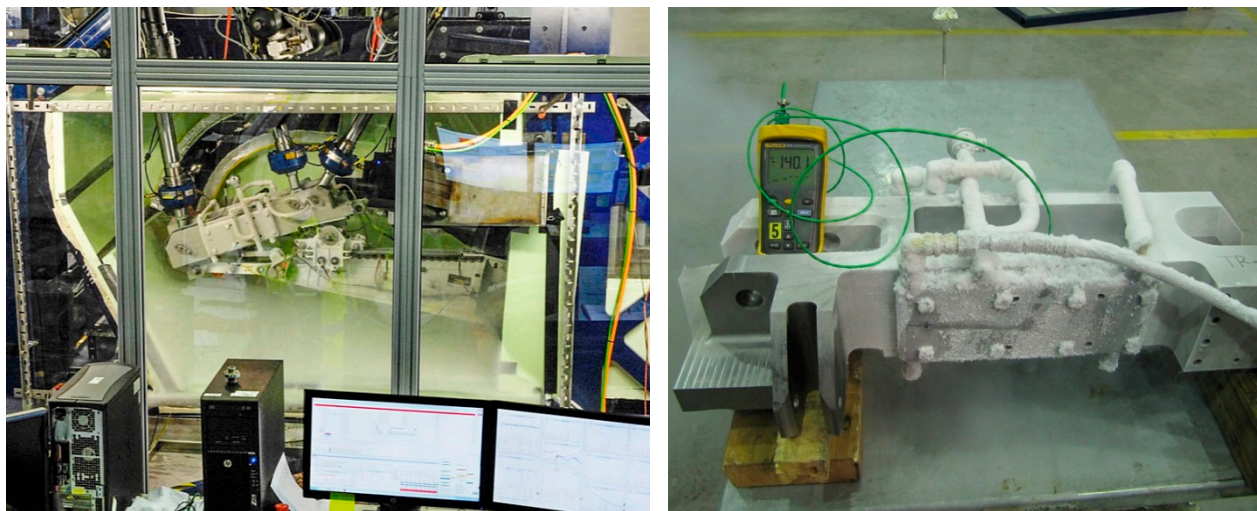


Figure 44: Full-scale endurance testing of flap tracks at  $-55^{\circ}\text{C}$  (left); thermal blocks, or heat sinks, are mounted on the LIDs to thermally insulate the test article from the test rig (right).

Some developmental problems have obviously been encountered. Since the endurance test is to run 24/7, hence unattended at night, a fully automated safety system is in place. At a particular night this system was triggered and the test was automatically shut-down. The next morning the operator on duty had significant problems of restarting the test. The circulation of the hydraulic oil in the shut-down condition turned out to be insufficient to prevent the oil from freezing up and blocking the flow. Additional oil heating elements were therefore included and the hydraulic actuators are monitored and electrically heated when necessary. This enables an easier restart after a cold shut-down and it also smoothens daily operation.

In order to prepare for possible future testing of space structures at very low temperatures, down to  $-180^{\circ}\text{C}$ , a prototype setup has been built to test an aluminium plate with a thickness, size and geometry equivalent to those of a segment of the Ariane Engine Thrust Frame (ETF). The test has been conducted successfully and it has demonstrated that the developed system is capable of cooling a representative structural component down to  $-180^{\circ}\text{C}$  in a reasonable amount of time.

### 8.3 Certification test activity for a hybrid structure

*Guido van Gool, Fokker Aerostructures*

Within the framework of the development of light-weight, hybrid CFRP-metal structures, a fatigue test has been conducted on a representative sub-assembly of a commercial airliner. This component test was part of the building block approach as defined in AC10-107B - see Figure 45.

The main objective of the test was to verify the fatigue and damage tolerance behaviour of the metal parts in the support structure. A total of 3x the Design Service Goal (DSG) has been applied using a flight-by-flight fatigue test spectrum. The fatigue test activities started with a shakedown. After the first DSG additional damages were applied in two subsequent damage tolerance intervals. The damage tolerance intervals consisted of one DSG each.

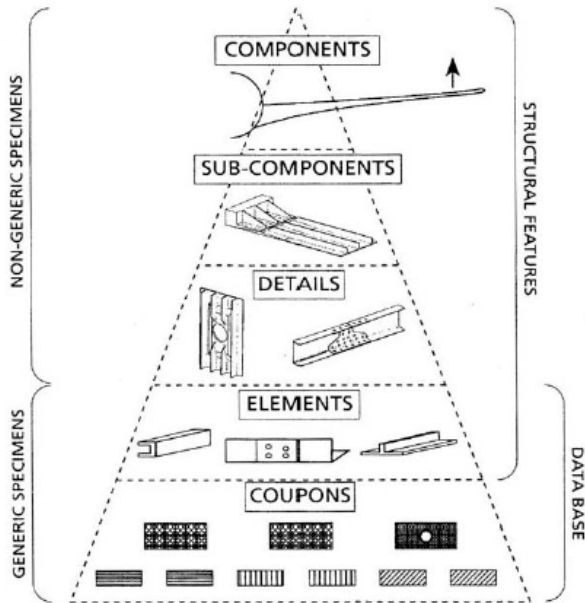


Figure 45: AC20-107B schematic diagram of building block tests.

The loading of a representative mix of flight profiles has been applied in the test. Thermal loads were not included. A Load Enhancement Factor (LEF) of 1.05 was added, which was to compensate for the absence of thermal loading and other forms of under-loading at local details and critical locations. The load spectrum values were multiplied by the LEF and subsequently the spectrum was truncated at about 80% limit load in order to avoid fatigue crack growth retardation effects.

The loads and deformations were applied by means of displacement controlled actuators at specific interface points. The air loads were simulated by means of a load controlled whiffle tree.

The specimen included several artificial damages in both the metal parts and CFRP structure. Damages in the CFRP structure were applied before the start of the test. The CFRP damages consisted of impacts up to BVID, delaminations and repairs.

For the metal parts artificial cracks were inflicted by means of special made saw blades. The width of the achieved saw cut was  $\sim 0.18\text{mm}$  using a sawblade of  $\sim 0.13\text{mm}$  thickness – see Figure 46.



Figure 46: Sawblade thickness.

A noteworthy detail is the direction of the saw cut. To ensure short crack initiation times a sharp notch at the saw cut tip was applied by inflicting a cut that was non-perpendicular to the surface (Figure 47).

All the component tests finished successfully. NDI did not reveal any unexpected crack or delamination propagation.

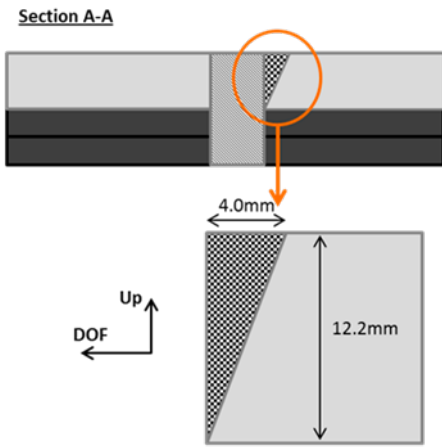


Figure 47: Non-perpendicular saw cut.

## 9 Fleet Life Management

### 9.1 Multi-nation NH90 Supportability Data Exchange

*Lex ten Have, John Dominicus, NLR*

Under contract of NAHEMA, NLR has developed and implemented a so-called NH90 Supportability Data Exchange (SDE) service for a consortium serving nine nations that operate the NH90/MRH90 helicopter. It consists of a common shared usage database and analysis toolbox with automated web based user data input.

The full NH90 SDE service comprises the following elements:

1. An Occurrence Reporting System (ORS) functionality which provides all participating nations with a capability to store, analyze, report and share NH90 SDE occurrence data in a flexible, secure environment, allowing adequate communication of occurrence reports between military headquarters, operational fields and maintenance facilities.
2. A Reliability Assessment System (RAS) functionality which provides the NH90 operator with the capability to determine experienced failure rates (MTBFs) of different helicopter components based on parts and equipment failures and maintenance task information. The SDE system contains provisions to extend reliability calculations towards Availability and Maintainability calculations, in the future.
3. An Aircraft Integrity Management (AIM) functionality which offers a threefold state-of-the-art structural integrity and fleet life management tool with a standard reporting facility. Input data for SDE AIM can be from different sources, e.g. MDS-GLIMS, Flight Data Recorder or a nation specific non-integrated retro-fit multi-channel data acquisition unit for strain gauge measurements, fed by data from the helicopter digital data buses.
4. A public and secure website (see: <https://sde.nlr.nl>), a moderated forum and a yearly users conference to evaluate and discuss integrity, completeness and validity of NH90 usage data, analysis results, helicopter degradation and maintenance, and to manage and direct necessary future SDE engineering support.

Physically, the NH90 SDE service is running on a 24/7 basis in a secure environment, located at NLR-Flevoland in the Netherlands.

In the past five years the participating nations have started uploading their occurrences and event data for RAM calculations. In May 2017 a 2<sup>nd</sup> five-year NAHEMA project phase is planned to be granted to NLR enabling SDE availability until 2022.

### 9.2 Roadmap to Condition Based Maintenance

*Lex ten Have, NLR*

In order to better understand worldwide developments in Condition Based Maintenance (CBM), NLR developed a Roadmap Condition Based Maintenance. It enables parties to position their high level goals and technical efforts in the wide field of CBM, PHM, SHM etc.

One of the goals is to identify CBM procedures that have already proven to be effective or economically attractive in one domain (e.g. military aerospace) and to try to translate these procedures towards other domains (e.g. renewable energy, rail & road transport, maritime, chemical industry etc.).

One of the outputs is a graphical presentation of the Roadmap CBM, see Figure 48.

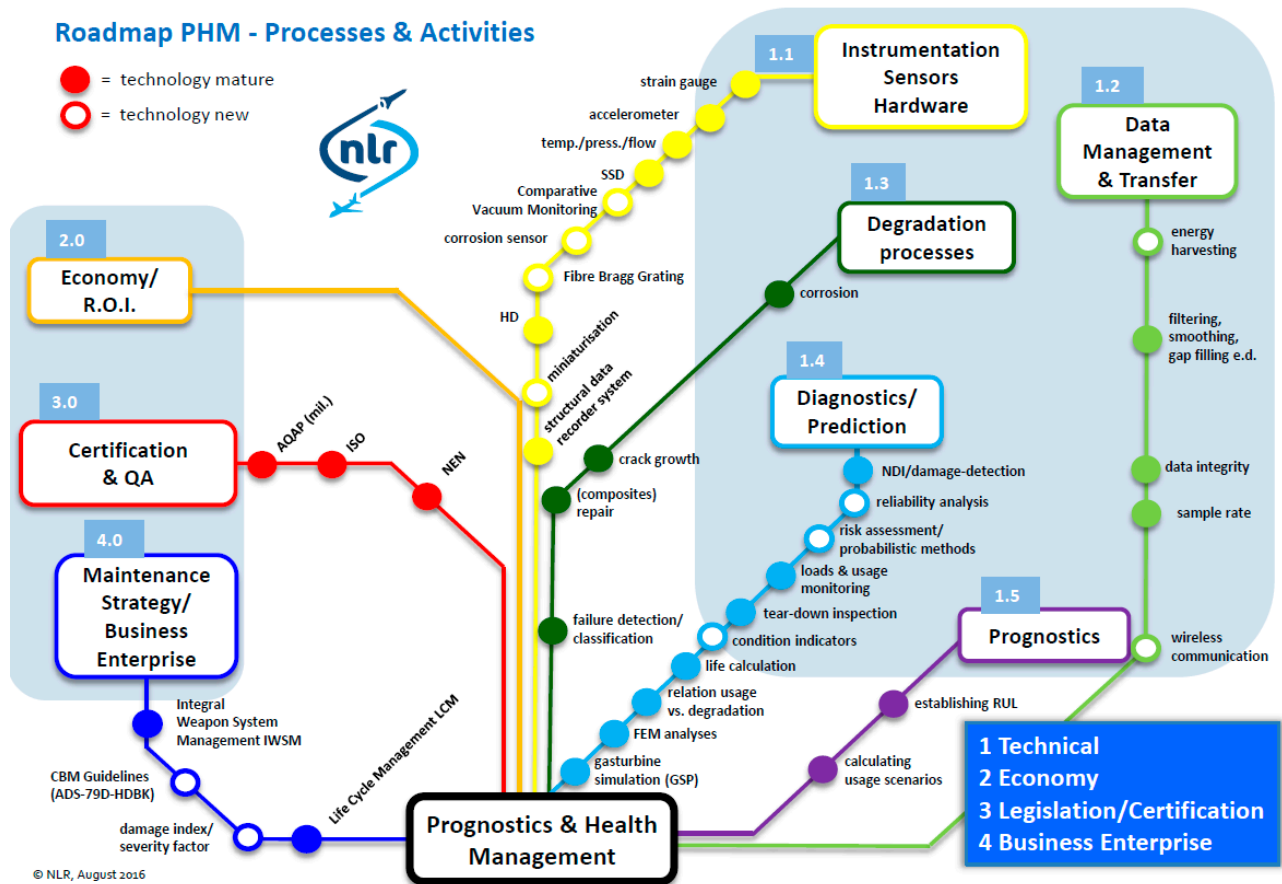


Figure 48: Roadmap CBM, as seen by NLR.

Another relevant issue that has been addressed within the Roadmap CBM study is the Technical Readiness Level (TRL) of certain aspects of CBM. As Figure 48 shows, four main fields have been identified: (1) Technical, (2) Economy, (3) Legislation/Certification and (4) Business Enterprise. The TRL levels associated with these 4 fields can be indicated by the bar chart in Figure 49.

Clearly, the most is going on (and has been achieved) in the technical field, linked to new hardware and software developments in sensors, data manipulation and algorithms, feature extraction, prognostics capabilities etc. The TRL levels reached in the technical area, by now, are considered relatively high with max TRL's of 7-9. Lower TRL levels still exist in the fields Economy, Legislation, Certification and Business Enterprise, and it is concluded by NLR that much more attention and focus is needed in these fields – see also section 7.1 of this National Review.

## Condition Based Maintenance – TRL levels Mil. Aerospace

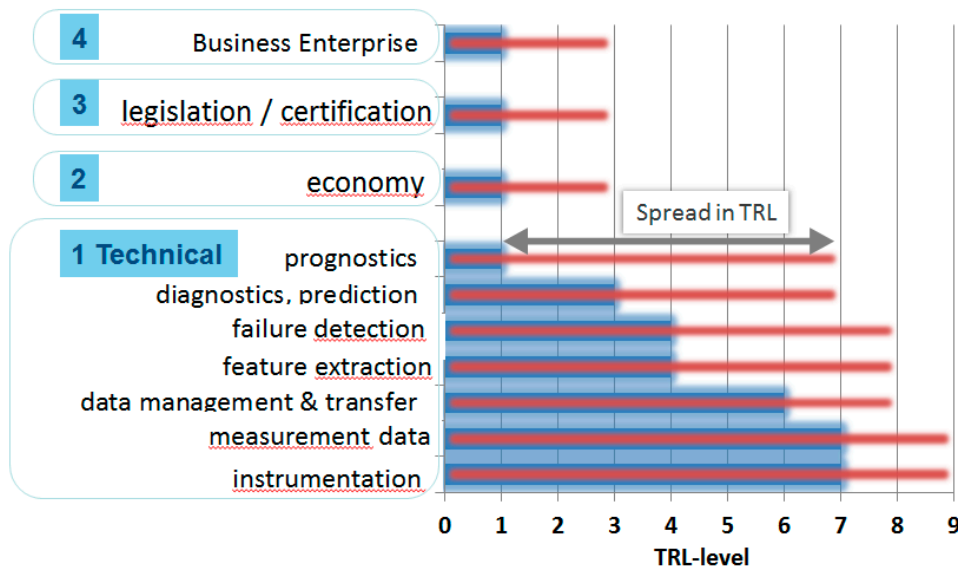


Figure 49: Technical Readiness Levels of CBM related topics.

## 9.3 Experimental investigation of damage tolerance substantiation methods for hybrid structures

Onno Bartels<sup>a</sup>, Tim Janssen<sup>b</sup>, Jaap Laméris<sup>a</sup>, <sup>a</sup>NLR, <sup>b</sup>Fokker Aerostructures

Structural components made out of metal require a different approach with respect to fatigue analysis, fatigue testing and structural health monitoring than components made out of fibre reinforced plastics. This leads to differences in the load spectra typically used for metals and composites, see Figure 50. For instance, occasional high loads can lead to crack growth retardation in metals. Thus, these are normally removed from a test spectrum in order to remain conservative. For composites however, removing these high loads from the test spectrum is unconservative since retardation effects do not occur in these materials. Additionally, to account for higher scatter in material properties, the loads in a composite fatigue test are typically increased by 10% - 20% by applying a Load Enhancement Factor (LEF), which further increases the gap between metal and composite load spectra. This makes the certification of composite-metal hybrid structures challenging, costly and time consuming.

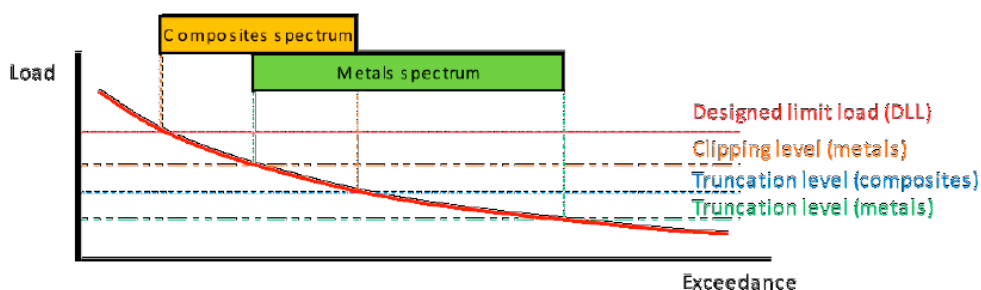


Figure 50: Difference between composite and metal load spectra.

In a FAA-JAMS sponsored study by NIAR, two methods that could potentially bridge the gap between the metal and composite load spectra have been proposed- see refs. [33] and [34].

The first method, LEF-Hybrid, employs different combinations of life- and load factors to manipulate a single load spectrum such that it can be used for metal-composite hybrid structures. Loads that would be increased beyond the metal clipping level after application of a LEF are repeated more often instead, whereas loads that are beyond the metal clipping level before applying a LEF are deferred toward the end of the test.

For the second method, Load-Life Shift (LLS), a fatigue test is performed in two phases. During the first phase, which is focused on the metal components, only a factor on life, not on loads, is applied. The second phase focuses on the composite components, and a LEF > 1.0 will be applied. If necessary, the metal components should be repaired or reinforced before this second phase, ensuring that no load redistribution takes place. During the first phase, the fatigue life of the composite components will be partially substantiated as well, which means that the duration of the second phase can be reduced. This could lead to a significant reduction in the required test duration.

These methods could reduce the required testing time and cost of a damage tolerance substantiation demonstration. However, more data is required to validate these methods. For this reason, an experimental study is currently being conducted by NLR and Fokker Aerostructures within the framework of GARTEUR Action Group SM/AG-35. Three sets of four identical double lap shear specimens are subjected to variable amplitude sequences: a reference sequence, a sequence generated using the LEF-Hybrid approach, and a sequence generated using the Load-Life shift approach. A comparison of the results from the LEF-Hybrid and the LLS sequences with the reference sequence will allow to draw conclusions on their validity for the tested material and failure mode.

A modified version of the FALSTAFF load sequence is used as reference. The mean level of the Shortened FALSTAFF spectrum has been lowered to ensure that sufficient damage is reached in the metal as well as in the CFRP parts. In order to obtain a reasonable testing time, an omission level of 30 % of limit load has been applied. An extensive durability and fatigue crack growth analysis has been conducted to show that the expected damage development would be equivalent to the full spectrum.

The tested specimens consist of a composite-aluminium double lap joint connection with lockbolts. The CFRP strip was impacted prior to the fatigue tests, since joints and impact sites are typical locations for fatigue damage to occur. Based on the results from an experimental impact programme, an energy level of 15 J was chosen to get sufficient BVID damage. The dimensions of the aluminium strips were chosen such that net stress failure would be the relevant failure mode.

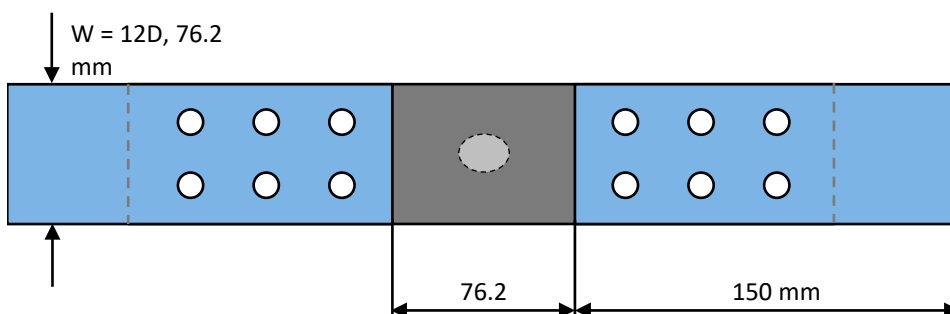


Figure 51: Schematic overview test specimen.

This is ongoing work. The results will be published upon completion of the study.

## 10 Special Category

### 10.1 Fatigue and fracture of Fibre Metal Laminates

*René Alderliesten, TU Delft*

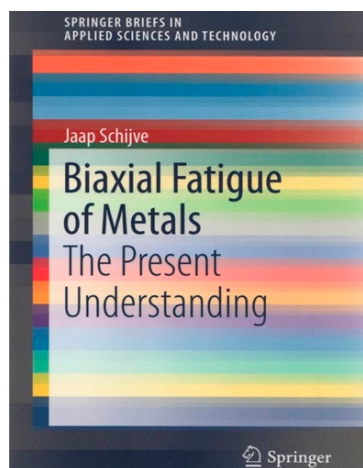
This year Springer will publish a book with the title *Fatigue and Fracture in Fibre Metal Laminates* [35]. This book contributes to the field of hybrid technology, describing the current state of knowledge concerning the hybrid material concept of laminated metallic and composite sheets for primary aeronautical structural applications. It is the only book to date on fatigue and fracture of fibre metal laminates (FMLs).

The first section of the book provides a general background of the FML technology, highlighting the major FML types developed and studied over the past decades in conjunction with an overview of industrial developments based on filed patents. The second section discusses the mechanical response to quasi-static loading, together with the fracture phenomena during quasi-static and cyclic loading. To consider the durability aspects related to strength justification and certification of primary aircraft structures, the third section discusses thermal aspects related to FMLs and their mechanical response to various environmental and acoustic conditions.

### 10.2 Biaxial fatigue of metals – the present understanding

*Jaap Schijve, TU Delft*

In 2016 Springer has published a so-called Springer Brief with the title *Biaxial Fatigue of Metals – The Present Understanding* [36]. Springer Briefs are concise booklets that focus on a single topic.



Problems of fatigue under multiaxial fatigue loads have been addressed in a large number of research publications. The present 23-page brief is primarily a survey paper of biaxial fatigue under constant amplitude loading on metal specimens. It starts with the physical understanding of the fatigue phenomenon under biaxial fatigue loads. Various types of proportional and non-proportional biaxial fatigue loads and biaxial stress distributions in a material are specified. Attention is paid to the fatigue limit, crack nucleation, initial micro-crack growth and subsequent macro-crack in different modes of crack growth. The interference between the upper and lower surfaces of a fatigue crack is discussed. Possibilities for predictions of biaxial fatigue properties are analysed with reference to the similarity concept. The significance of the present understanding for structural design problems is considered. The paper is completed with a summary of major observations.

### 10.3 Portable Impactor

*Rens Ubels, Paul Arendsen, NLR*

NLR has developed an accurate portable impactor system that can be used to inflict impact damages to composite structure in full-scale fatigue test articles. The achievable impact energies range from 12 to about 150 J. The available impact tups have diameters of 0.5 inch, 1.0 inch and 16 mm. A flat tup with a diameter of 0.5 inch is also included. A

velocity measurement device is installed at the exit side of the guidance tube, which connects to a National Instruments data acquisition box. A catching device prevents multiple impacts.

The system is already in use within NLR, Bombardier, Textron Aviation and Korea Aerospace Industries.

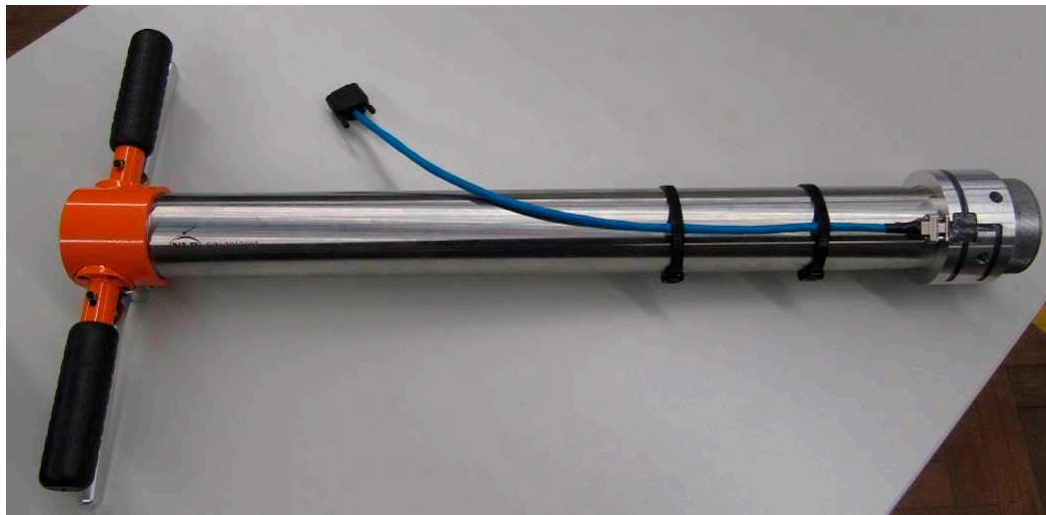


Figure 52: Portable impactor with velocity measurement device at the end of the barrel.

## 10.4 Delft Workshop on Physics of Fatigue Damage Growth

10-11 October 2016, TU Delft Science Centre, Delft, The Netherlands

TU Delft organised a workshop on the physics underlying the current empirical approaches to understanding fatigue crack growth. The aim of this workshop was to facilitate discussion between a small group of invited experts. Approximately 20 people were invited to participate in this 1.5-day workshop with expertise ranging from fatigue in metals to fatigue in composites.

It was generally agreed that phenomenologically there are similarities between different materials, i.e. similar R-effects, and data results in sigmoidal, non-linear shapes with empirical Paris-type curves. The physical micro-mechanisms for fatigue crack initiation and growth do not seem to be well understood yet, neither for metals nor for composites. Due to their morphology, there is dissimilarity between metals and composites with respect to the types of damage mechanisms and likely also to geometrical scales on which these mechanisms act, but there is very little information available on the relevant times scales on which the microscopic mechanisms act.

## 10.5 Milestone case histories in aircraft structural integrity

Russell Wanhil<sup>a</sup>, Loris Molent<sup>b</sup>, Simon Barter<sup>b</sup>, <sup>a</sup>NLR, <sup>b</sup>DST-G

In a joint collaborative effort, NLR in the Netherlands and DST-G in Australia have published an overview of milestone case histories in aircraft structural integrity [37].

## References

- [1] Hogeveen J (2016), Towards a proper understanding of fatigue crack growth and crack closure, MSc thesis, TU Delft.  
<http://repository.tudelft.nl/islandora/object/uuid:bf64c0eb-fc2d-4e3a-90ed-696071625606/datastream/OBJ/download>
- [2] Amsterdam E, Grooteman FP (2016), The influence of stress state on the exponent in the power law equation of fatigue crack growth. *International Journal of Fatigue* 82, 572-578.
- [3] Michielssen J (2017), Fatigue crack growth in selective laser melted Ti-6Al-4V, MSc thesis, Delft University of Technology.  
<http://repository.tudelft.nl/islandora/object/uuid:c62fc3a4-6aea-4180-b125-ac54fede0762/datastream/OBJ/download>
- [4] Pascoe JA (2016), Characterisation of Fatigue Crack Growth in Adhesive Bonds, PhD dissertation, TU Delft.  
<http://repository.tudelft.nl/islandora/object/uuid%3Aebbf552a-ce98-4ab6-b9cc-0b939e12ba8b?collection=research>
- [5] Pascoe JA, Alderliesten RC, Benedictus R (2017), On the physical interpretation of the R-ratio effect and the LEFM parameters used for fatigue crack growth in adhesive bonds, *International Journal of Fatigue* 97, 162–176.  
<http://www.sciencedirect.com/science/article/pii/S0142112316304406>
- [6] Pascoe JA (2016), Research data: <http://data.4tu.nl/repository/resource:repository/object/search?q=pascoe&n=20>
- [7] Teixeira de Freitas S, Sinke J (2017), Failure analysis of adhesively-bonded metal-skin-to-composite-stiffener: Effect of temperature and cyclic loading. *Composite Structures* (166): 27–37.
- [8] Wang W (2017), Multiple Site Damage crack growth behaviour in Fibre Metal Laminate Structures, PhD dissertation, Delft University of Technology.
- [9] Gupta W (2017), Directionality of damage growth in Fibre Metal Laminates and Hybrid Structures, PhD dissertation, Delft University of Technology.
- [10] Müller B, Anisimov AG, Sinke J, and Groves RM (2015), Thermal strains in heated fibre metal laminates. *Proceedings of the ETNDT: Emerging Technologies in Non-Destructive Testing VI*, 6, 205 – 211.
- [11] Liu P, Yao L, Groves RM (2015), Near-infrared optical coherence tomography for the inspection of fibre composites, *Proc. 7th International Symposium on NDT in Aerospace*, Bremen
- [12] Liu P, Groves RM, Benedictus R (2014), 3D monitoring of delamination growth in a wind turbine blade composite using Optical Coherence Tomography, *NDT & E International*
- [13] Narayana Swamy JK, Lahuerta F, Anisimov AG, Nijssen RPL, Groves RM (2016), Evaluating delamination growth in composites under dynamic loading using infrared thermography. In K Drechsler (ed.). *Proceedings of the 17th European Conference on Composite Materials: Munich, Germany, 26-30 June*.
- [14] AC 120-104 (2011), Establishing and Implementing Limit of Validity to Prevent Widespread Fatigue Damage, January 10.
- [15] White, FM (2006), *Viscous Fluid Flow*, McGraw-Hill, Third Edition, International Edition, pp. 42, 547.
- [16] Kurganov, VA (2011), Adiabatic Wall Temperature, *Thermopedia*, 3 February.
- [17] Huth, H (1984), Zum Einfluß der Nietnachgiebigkeit mehrreihiger Nietverbindungen auf die Lastübertragungs- und Lebensdauervorhersage, Dissertation, TU Munich.
- [18] Stubbs, N, Farrar, CR (1995), Field Verification of a Nondestructive Damage Localization and Severity Estimation Algorithm, *Proc. of 13th IMAC*, 210-218.

- [19] Ooijevaar, TH, Warnet, L, Loendersloot, R, Akkerman, R, Tinga, T (2016) Impact Damage Identification in Composite Skin-Stiffener Structures Based on Modal Curvatures, *Structural Control & Health Monitoring*, 23(2), 198-217.
- [20] Bos, MJ (2015), Fielding a Structural Health Monitoring system on legacy military aircraft: A business perspective, *Journal of the Korean Society for Nondestructive Testing*, Vol 35, No 6: 421-428.
- [21] Hwang JS, Müller JM, Loendersloot R, Tinga T (2017), Modal Strain Energy Based Structural Health Monitoring Validation on Rib Stiffened Composite Panels, NLR Technical Publication NLR-TP-2017-061.
- [22] Hwang, JS, Loendersloot, R, Tinga, T (2015), Experimental evaluation of vibration-based damage identification methods on a composite aircraft structure with internally-mounted piezodiaphragm sensors, 10th International Workshop on Structural Health Monitoring (IWSHM), Stanford University, CA, September 1-3, NLR Technical Publication NLR-TP-2015-196.  
<http://reports.nlr.nl:8080/xmlui/handle/10921/1070>
- [23] Bos MJ, Wanhill RJH (2011), Review of aeronautical fatigue investigations in the Netherlands during the period March 2009 - March 2011, NLR Technical Publication NLR-TP-2013-123.  
<http://reports.nlr.nl:8080/xmlui/handle/10921/121>
- [24] Bos MJ (2013), Review of aeronautical fatigue investigations in the Netherlands during the period March 2011 - March 2013, NLR Technical Publication NLR-TP-2013-158.  
<http://reports.nlr.nl:8080/xmlui/handle/10921/966>
- [25] Bos MJ, Habets GMHJ (2015), Review of aeronautical fatigue investigations in the Netherlands during the period March 2013 - March 2015, NLR Technical Publication NLR-TP-2015-123.  
<http://reports.nlr.nl:8080/xmlui/handle/10921/1001>
- [26] Bos MJ, Hwang JS, Grooteman FP, Park CY (2013), Load Monitoring and Structural Health Monitoring within the Royal Netherlands Air Force, NLR Technical Publication NLR-TP-2013-479.  
<http://reports.nlr.nl:8080/xmlui/handle/10921/965>
- [27] Have AA ten et al (2012), FLM support for the NH90 community, NLR Technical Publication NLR-TP-2012-556.  
<http://reports.nlr.nl:8080/xmlui/handle/10921/506>
- [28] Bos MJ (2012), Lockheed C-130H(-30) Fleet Life Management within the Royal Netherlands Air Force, NLR Technical Publication NLR-TP-2012-415.  
<http://reports.nlr.nl:8080/xmlui/handle/10921/498>
- [29] Oldersma A, Bos MJ (2011), Airframe loads & usage monitoring of the CH-47D helicopter of the Royal Netherlands Air Force, NLR Technical Publication NLR-TP-2011-033.  
<http://reports.nlr.nl:8080/xmlui/handle/10921/114>
- [30] Winkel FC te, Spiekhout DJ, RNLAF F-16 Loads & Usage Monitoring Program, NLR Technical Publication NLR-TP-2002-309.  
<http://reports.nlr.nl:8080/xmlui/handle/10921/694>
- [31] Bos MJ, Oldersma A, Jongstra J, Verheem FJA (2015), Towards Condition Based Maintenance of Aging Military Helicopters, NLR Technical Publication NLR-TP-2015-139.  
<http://reports.nlr.nl:8080/xmlui/handle/10921/1012>
- [32] Kan WJ van, Tijs BHAH, Jong GJ de, Frel HC de, Singh NK (2016), Strength of notched and unnotched thermoplastic composite laminate in biaxial tension and compression, *Journal of Composite Materials*, Vol. 50(25) 3477–3500.
- [33] Tomblin JS, Seneviratne WP (2011), Determining the Fatigue Life of Composite Aircraft Structures Using Life and Load-Enhancement Factors, DOT/FAA/AR-10/6.

- [34] Seneviratne WP, Tomblin JS (2014), Certification of Composite-Metal Hybrid Structures using Load-Enhancement Factors, FAA Joint Advanced Materials and Structures (JAMS), Seattle, WA.
- [35] Alderliesten, RC (2017), Fatigue and Fracture of Fibre Metal Laminates, Springer Netherlands.
- [36] Schijve J (2016), Biaxial Fatigue of Metals – the Present Understanding, Springer Brief, Springer Netherlands.
- [37] Wanhill RJH, Molent L, Barter S (2016), Milestone case histories in aircraft structural integrity. In: "Reference Module in Materials Science and Materials Engineering", editor-in-chief S. Hashmi, Elsevier Inc., Oxford, UK, pp. 1-19.

*This page is intentionally left blank.*



**NLR**

Anthony Fokkerweg 2

1059 CM Amsterdam, The Netherlands

p) +31 88 511 3113 f) +31 88 511 3210

e) [info@nlr.nl](mailto:info@nlr.nl) i) [www.nlr.nl](http://www.nlr.nl)